*Petrology, Vol. 12, No. 6, 2004, pp. 540–560. Translated from Petrologiya, Vol. 12, No. 6, 2004, pp. 609–631.*


# Archean Eclogites in the Belomorian Mobile Belt, Baltic Shield

**O. I. Volodichev*, A. I. Slabunov*, E. V. Bibikova**, A. N. Konilov***, and T. I. Kuzenko***

**Institute of Geology, Karelian Research Center, Russian Academy of Sciences, Pushkinskaya ul. 11, Petrozavodsk, 185610 Karelia, Russia*
*e-mail: volod@krc.karelia.ru*
***Vernadsky Institute of Geochemistry and Analytical Chemistry, Russian Academy of Sciences, ul. Kosygina 19, Moscow, 117925 Russia*
*e-mail: bibikova@geokhi.ru*
****Geological Institute, Russian Academy of Sciences, Pyzhevskii per. 7, Moscow, 109017 Russia*
*e-mail: konilov@geo.tv-sign.ru*

Received March 19, 2003

**Abstract**—Eclogites of Archean (2720 ± 8 Ma) and Proterozoic (2416.1 ± 1.3 Ma) age were found in the Belomorian Mobile Belt of the Baltic Shield near the village of Gridino in Karelia. The unique Archean eclogites described in this paper and the symplectitic apoeclogitic rocks that developed after them in the course of their retrogression are components of a complicated polygenetic chaotic complex, which is thought to be composed of extensively migmatized rocks of a tectonic melange zone. The eclogite-bearing complex is cut by gabbronorite dikes (2.43–2.44 Ga) and small plagiogranite intrusions and veins (which were dated by the U–Pb zircon method at 2701.3 ± 8.1 Ma in Stolbikha Island). Zircons from the symplectitic apoeclogites were dated by the U–Pb method on a NORDSIM ion microprobe at the Archean (2720 ± 8 Ga). The petrochemical characteristics of the eclogites are comparable with those of metabasalts (amphibolites) of the ophiolite-like complex in the Central Belomorian Mafic Zone. This paper reports the results of the detailed geological, petrological, and mineralogical examination of the complex and the *P–T* metamorphic parameters of the eclogites during their prograde and retrograde metamorphic evolution. The prograde metamorphism ($P$ = 14.0–17.5 kbar, $T$ = 740–865°C) of the eclogites occurred in a geodynamic environment in which the processes of "warm" subduction could take place. The trajectory of the multistage subisothermal decompression during the retrograde stage with the pressure decreasing from 14.0 to 6.5 kbar at $T$ = 770–650°C was controlled by the exhumation of the eclogites.

## INTRODUCTION

The problem of eclogites as high-pressure (HP) and ultrahigh-pressure (UHP) rocks continuously attracts keen interest of geologists, which was significantly whetted lately in the context of the plate tectonic theory (Godard, 2001). According to this concept, eclogites were formed in Phanerozoic orogenic belts in relation to the subduction of crustal rocks and the later exhumation of crustal fragments during the development of accretionary and collisional processes. The possibility of plate tectonics in the Archean is commonly doubted because of the absence of eclogites, one of the main indicators of deep subduction, from geological complexes of this age. The high geothermal gradient in the relatively thin Archean crust is believed (Green, 1975; Baer, 1977; and others) not to be able to produce eclogites, and it was supposedly not until the Proterozoic (~1000 Ma) that conditions in the lithosphere became suitable for the origin of these rocks. There are only a very few publications mentioning eclogites for which an Archean age was proposed: one of them was in Glenelg, Scotland (Alderman, 1936) and the other in the Snowbird tectonic zone in Canada (Percival, 1994). However, their ancient age was not confirmed by isotopic dates. Moreover, geological–geochronological evidence recently obtained on the Kramanituar Complex, a segment of the Snowbird tectonic zone (Sanborn-Barrie *et al.*, 2001), demonstrates that the nearly synchronous processes of gabbro–anorthosite magmatism, deformations, and HP metamorphism were related there to the Paleoproterozoic (1.9 Ga) reactivation of the Archean structure, and the culmination of the eclogite-facies metamorphism in the rocks of the Glenelg–Attadeil inlier has a Sm–Nd age of ~1.08 Ga and, thus, can be correlated with the Grenville orogeny (Storey *et al.*, 2003).

At the same time, the Belomorian Mobile Belt was reportedly affected by three episodes of HP metamorphism: in the Late Archean (>2.7 Ga), Early Proterozoic (~2.45 Ga), and Early Proterozoic–Svecofennian (1.9–1.8 Ga) (Volodichev, 1990). Eclogites were found near the village of Gridino (Fig. 1), along with eclogite-

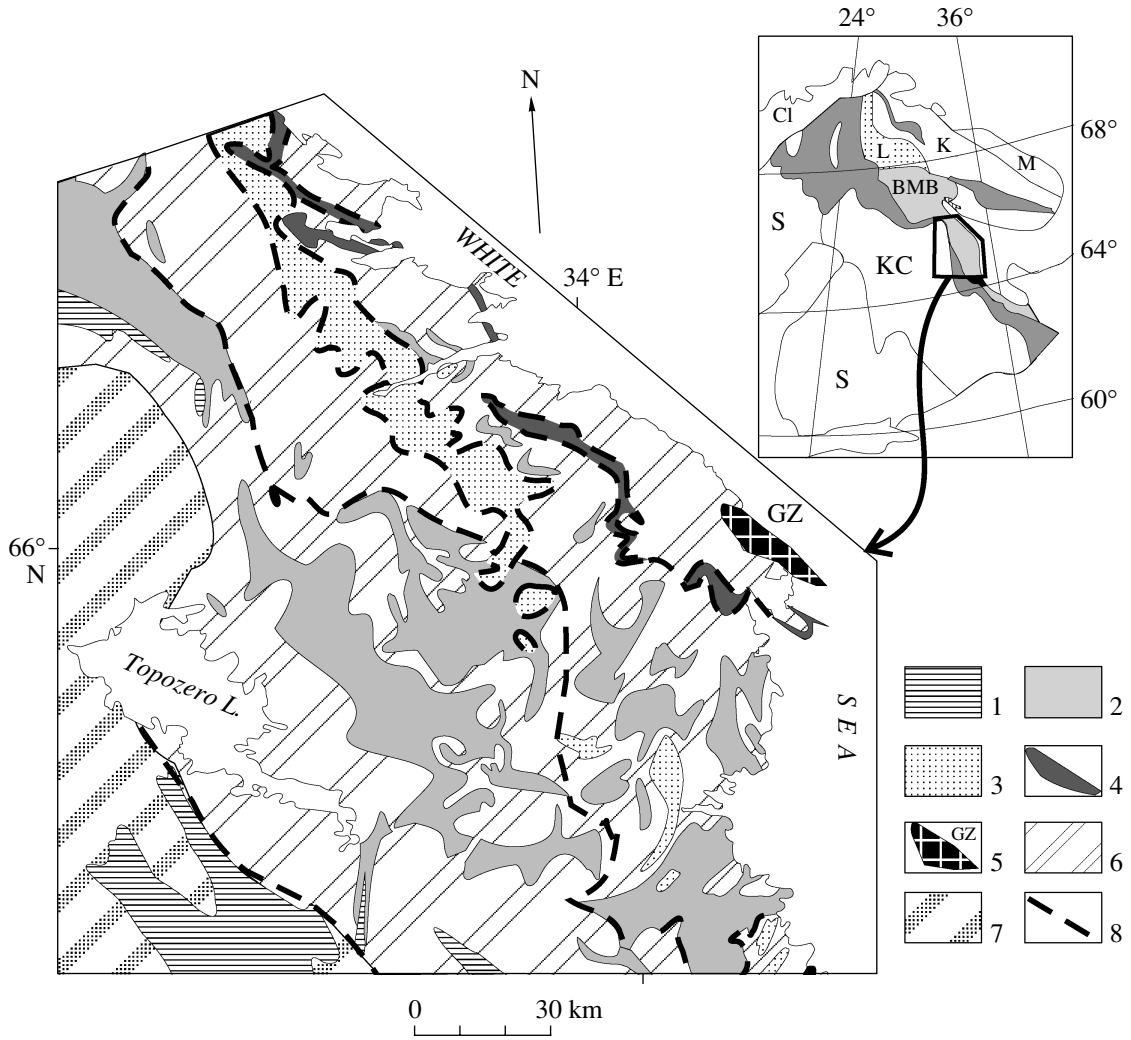


**Fig. 1.** Schematic geological map of northern Karelia. (1) Early Proterozoic (2.5–1.92 Ga) supracrustal rocks; (2) Late Archean (2.9–2.82 and 2.8–2.78 Ga) greenstone complexes; (3) "aluminous" gneisses; (4) Late Archean (2.88–2.85 Ga) amphibolites and ultrabasites of the Central Belomorian Mafic Zone; (5) extensively migmatized zone of tectonic melange near the village of Gridino with fragments of altered eclogites (GZ); (6) gneissose granitoids and migmatites of the BMB (2.9–2.7 Ga); (7) granitoids of the Karelian craton (3.2–2.7 Ga); (8) inferred overthrusts.

The inset demonstrates major geologic structures in the eastern Baltic Shield and the location of the study area: M—Murmansk craton, K—Central Kola Domain, L—Lapland Granulite Belt, BMB—Belomorian Mobile Belt, KC—Karelian Craton, S—Svecofennides, Cl—Caledonides.

like rocks and their kyanite-bearing varieties (symplectitic apoeclogites) of two distinct ages: Late Archean and Early Proterozoic (Volodichev, 1977, 1990, 1997). This paper reports geological and petrological characteristics and isotopic dates of these Archean eclogites. This seems to be the world's first trustworthy find of such rocks in Late Archean metamorphic complexes.

## GEOLOGY OF THE COMPLEX

The eclogites and the products of their extensive retrogression are constituents of a complicated polygenetic chaotic complex, which occurs as a linear structure trending northwestward and exposed as a 6- to 7-km-wide stripe in the shore of the White Sea and on some islands from Velikaya Bay in the northwest to the Ivanovy Ludy Islands in the southeast (Fig. 1). These rocks contrastingly differ from the tonalitic gneisses cropping out northeast of the stripe and from the heterogeneous complex of amphibolites and tonalitic and aluminous gneisses in the southwest, although their relationships are still not absolutely clear. The composition and ratios of components in the rocks of this complex are comparable with those in the field of migmatites of the agmatite type, in which the migmatizing granitoid magma fills and traces a preexisting zone of tectonic melange.

The vein constituent of this complex is of injection–magmatic nature and consists of gneissose granites,

whose composition corresponds to tonalite, plagiogranite, or, more rarely, diorite. The multiple structural–metamorphic recycling of the granitoids transformed them into gneisses of predominantly biotite–amphibole composition, often with garnet and, sometimes, clinopyroxene. The relict massive varieties pervasively contain corona glomeroblasts, consisting of garnet, clinopyroxene, amphibole, and biotite, which seem to replace orthopyroxene. These indirect indications and finds of relict orthopyroxene in granitoids on First Kokkov Island suggest that the vein material of the migmatites could be of enderbitic composition.

Another constituent of the chaotic complex is numerous rounded or, rarely, podiform fragments, which are unevenly distributed in the gneiss-granitic material and whose size varies from a few dozen centimeters to a few meters across. The fragments consist of rocks of different composition, genesis, and age, which affiliate with different associations and were produced at different depths. Some of the fragments are variably reworked eclogites.

The amounts of rock fragments in the chaotic complex broadly vary and average 25–30% of the overall rock volume. Although the fragments have different compositions, they are strongly dominated by mafic rocks, which are variably transformed eclogites, garnet, garnet–clinopyroxene, and feldspathic amphibolites, and metagabbroids of different composition (which belong to the tholeiitic and ferrotholeiitic series) and age. Eclogites are preserved in the form of relics among garnet–clinopyroxene–plagioclase rocks with amphibole and quartz. The latter rocks are diablastic and contain symplectites of clinopyroxene and plagioclase, which testify that the rocks developed after eclogites during decompression. The symplectitic eclogites were subsequently transformed into clearly banded garnet–clinopyroxene and garnet amphibolites and, sometimes, into feldspathic rocks with plagioclase pseudomorphs after garnet.[1] This character of transformations in the eclogites does not imply that all amphibolites occurring in this suite of rock fragments are modified eclogites. Along with the predominant metabasites, some fragments are metamorphosed ultramafics. Eclogitized pyroxenites were found in Vorotnaya Luda Island. A typical component of the fragments is zoisite and banded amphibole–zoisite granofels. The former rocks are dominated by white or pistachio-green zoisite with subordinate amounts of quartz, calcic plagioclase, carbonate, and secondary epidote. The amphibole–zoisite rocks additionally contain amphibole and, sometimes, younger garnet. Rare rock fragments consist of gneisses, including aluminous varieties, such as kyanite–garnet–biotite gneisses exposed on Cape Kirbei, and calciphyres with amphibole (which probably replaces olivine), exposed near the village of Gridino.

[1] Together with the equigranular *Grt–Cpx–Pl* crystalline schists, these rocks were previously referred to as eclogite-like rocks (Volodichev, 1977, 1990).

The textures of these rocks were variably modified during the pre-migmatite stage. Some of the rocks preserved their massive textures, while others (including the eclogites) are extensively deformed and folded into isoclinal folds of, likely, more than one age generations. The petrochemistry of the rock fragments suggests that the eclogites and their derivatives correspond to basites ($SiO_2$ = 47–51 wt %, $Na_2O + K_2O$ = 1.38–4.3 wt %) of the tholeiite series (FeO*/MgO = 0.5–2.5). The REE contents of the rocks are 2–12 times higher than in chondrites (Sun, 1982), and the REE patterns are flat or weakly fractionated ($La_N/Sm_N$ = 0.99–1.8, $Gd_N/Yb_N$ = 0.77–1.17). These rocks can be readily paralleled with the metabasalts (amphibolites) of the ophiolite-like complex in the Central Belomorian Mafic Zone (Slabunov and Stepanov, 1998; Bibikova *et al.*, 1999). These similarities are further accentuated by the fact that the eclogites that developed after metapyroxenites (Vorotnaya Luda Island) have analogues among the rocks of this complex. The amphibolites (except their leucocratic varieties) have petrochemical characteristics similar to those of the eclogites. The zoisite and banded amphibole–zoisite rocks are obviously former anorthosites and gabbro-anorthosites metamorphosed under *P–T* conditions close to those of the eclogites. The kyanite–garnet–biotite gneisses in lenticular bodies in Cape Kirbei are somewhat distinct petrographically, but their petrochemical characteristics are close to those of the aluminous gneisses widespread in the BMB.

The great diversity of rocks in the fragments, their genetic and petrochemical characteristics in the structure as a whole and its parts or even in individual exposures, variable fragmentation of the rocks and their variable role in the deformations, significant metamorphic gradients of individual constituents of the complex, and, finally, the obvious differences of these rocks from the rocks composing adjacent structures provide evidence of the significant disintegration and displacement of the protolithic components, which were, in fact, an allochthonous mixture. This suggests that the migmatite field marks a tectonic zone, which was produced during the pre-migmatite stage and shows certain features of a tectonic melange zone. These features include rare finds of rock fragments that could be the probable protolith of the tectonic melange matrix: melanocratic garnet–biotite gneisses cementing fragments of garnet–clinopyroxene amphibolites and schistose garnet amphibolites in a cement of small metapyroxenite fragments, as well as leucocratic amphibolites and mesocratic amphibole–biotite gneisses that occur as small lenticular banded bodies in the matrix among the gneiss-granites.

Thus, the Archean eclogite-bearing chaotic complex of the Gridino zone is extensively migmatized tectonic melange, which was significantly reworked by overprinted deformation and metamorphic processes.

**Table 1.** U–Pb isotopic data on zircons from plagiogranite (sample 2913-6)

| no. | Size fraction, μm | Sample, mg | Concentration, ppm | | Pb isotopic composition | | | Isotopic ratios | | Isotopic age, Ma ±σ |
|---|---|---|---|---|---|---|---|---|---|---|
| | | | U | Pb | $^{206}Pb/^{204}Pb$ | $^{206}Pb/^{207}Pb$ | $^{206}Pb/^{208}Pb$ | $^{206}Pb/^{238}U$ | $^{207}Pb/^{235}U$ | $^{207}Pb/^{206}Pb$ |
| 1 | +100, 5 crystals | 0.0316 | 83.29 | 44.49 | 15000 | 5.6088 | 5.997 | 0.4618 | 11.3130 | 2631.3 ± 1.8 |
| 2 | 4 colorless crystals | 0.0292 | 81.88 | 38.917 | 3370 | 5.652 | 11.22 | 0.4346 | 10.39745 | 2591.6 ± 1.9 |
| 3 | 4 crystals | 0.0223 | 54.81 | 29.93 | 1050 | 5.333 | 5.059 | 0.4535 | 11.0089 | 2616.2 ± 2.0 |
| 4 | +150, 1 crystal | 0.0564 | 111.15 | 66.29 | 5870 | 5.497 | 3.743 | 0.4768 | 11.8379 | 2653.2 ± 1.8 |
| 5 | –75 | 0.020 | 101.06 | 50.975 | 2544 | 5.3779 | 7.147 | 0.4407 | 11.0205 | 2665.5 ± 1.9 |

Note: Zircon isotopic study was conducted according to (Krogh, 1973) for small zircon samples. The U and Pb concentrations were determined by isotopic dilution using a mixed $^{205}Pb + {}^{233}/^{236}U$ tracer. The blank was 0.02 ng for Pb. The isotopic composition was measured on a Finnigan MAT 261 multicollector solid-source mass spectrometer at the Isotopic laboratory of the National Museum of Natural History in Stockholm. The isotopic ages were calculated by the program (Ludwig, 1991). The errors in the U–Pb ratios were 0.3%. A correction for common Pb was introduced for an age of 2700 Ma in compliance with the model (Stacey and Kramers, 1975). The isotopic age corresponding to the upper intercept of the discordia and concordia is 2701.3 ± 8.1 Ma, the lower intercept yields 1083 ± 60 Ma.

## AGE OF THE ECLOGITES

Geological evidence unambiguously constrain the upper age limit of the chaotic complex.

First of all, gabbro-norite dikes belonging to the Early Proterozoic lherzolite–gabbronorite complex (Stepanov, 1990) with an age of 2.43–2.44 Ga (Lobach-Zhuchenko *et al.*, 1998; Slabunov *et al.*, 2001) cut the rocks of the complex and often have chill zones in contact with them. Second, the complex is intersected by small plagiogranite intrusions (Berezhnye Islands) and veins (Stolbikha Island), as well as veins of plagioclase–microcline granites (Cape Dmitriev), which intruded the already gneissose and remetamorphosed migmatite complex. For example, a steep undeformed plagiogranite vein up to 60 cm thick exposed on Stolbikha Island (Fig. 2) and was traced for 20 m cuts across the gneissosity of the gneiss-granite and an amphibolite fragment.

This vein was sampled for the purposes of geochronology (sample 2913-6). The accessory zircons from this rock are euhedral transparent pale crystals (Fig. 3), which are strongly fractured. The grains selected for dating were the least faulty. The results are summarized in Table 1 and Fig. 3. As can be seen from the table, the U contents in the zircons are very low, usually less than 100 ppm, but the age values are nevertheless significantly discordant. The age corresponding to the upper intercept of the discordia and concordia is 2701 ± 8.1 Ma, and this estimate was assumed as the crystallization age of the zircon. Considering its magmatic genesis, this value can also be taken as the crystallization age of the granite vein. The lower intercept of the discordia and concordia corresponds to an age close to 1000 Ma and can be caused by double Pb loss in Svecofennian and modern time, a process facilitated by the extensive fracturing of the zircon crystals. In this interpretation, the age of 2701 Ma is the minimum age limit for the granite.

With regard for the geological setting of the plagiogranites, their dates suggest that the eclogite-bearing chaotic complex was produced in the Late Archean, no earlier than 2701 Ma, before the emplacement of the postkinematic veins.

Other rocks selected for isotopic dating were those of the eclogite group itself: symplectitic apoeclogite (sample 2913-11 or V-3-1) and eclogites (sample 2913-12 or V-3) from a fragment in gneiss-granites of Stolbikha Island (Fig. 2).

We managed to obtain a small amount (~1 mg) of zircon from sample 2913-11. The zircon occurs as equant transparent colorless grains without zoning and with rich faceting (Fig. 4). Zircon crystals of this type crystallize under high pressures and are characteristic of high-pressure granulites and eclogites (Masamichi and Hi, 1983; Bibikova, 1989).

The U–Th–Pb isotopic analyses of the zircons were conducted at the Laboratory of Isotopic Geology of the Swedish Museum of Natural History in Stockholm on a Cameca-1270 ion microprobe (NORDSIM). The zircon grains to be analyzed and the zircon standard were prepared as epoxy pellets that were polished until the cores of the crystals were exposed. Preparatory to the analyses, the pellet was sputter coated with gold. The primary ion beam consisted of negatively charged oxygen ions ($O^{-2}$) that bombarded an ellipsoidal area at the crystal surface 25 × 40 μm in size. The secondary ions were analyzed at a resolution of 5600, which made it possible to reliably differentiate between all atomic masses of interest. The reader can find more detailed descriptions of this method in (Whitehouse *et al.*, 1997; Wiedenbeck *et al.*, 1995). The Pb isotopic composition and the U/Pb isotopic rations were measured accurate to 0.1–0.3 and 1–3%, respectively. The results are presented in Table 2 and the diagrams of Fig. 4.

The zircons are characterized by extremely low contents and an even distribution of radioactive elements.

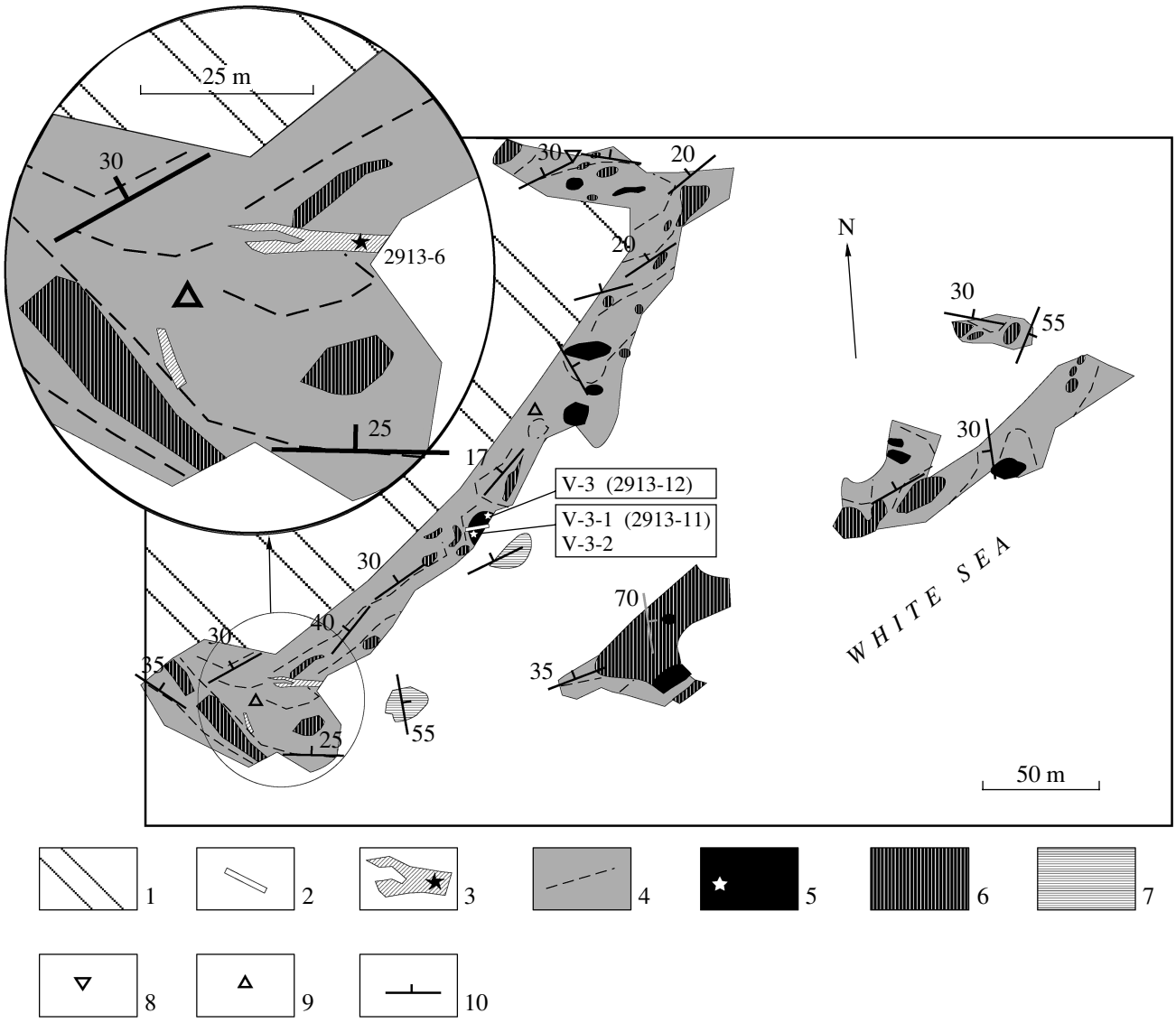


**Fig. 2.** Schematic geological map of the southeastern part of Stolbikha Island (prepared by A.I. Slabunov and O.S. Sibelev). Inset: crosscutting plagiogranite veins and the sampling site of geochronologic sample 2913 (marked with an asterisk).

(1) Quaternary deposits; (2) pegmatite vein; (3) late Archean (2701 ± 8 Ma) plagiogranite; (4) gneiss-granite, dashed lines show generalized directions of the gneissosity; (5) eclogite and symplectitic apoeclogite, site of petrological and geochronological sampling (sample 2913-11); (6) amphibolite; (7) leucocratic amphibolite; (8–9) occurrences of (8) zoisite and (9) ultramafic rocks (not to scale); (10) strikes and dips (numerals) of the gneissosity and banding.

In a concordia diagram (Fig. 4a), almost all of the analyzed points yield concordant age values. The average $^{207}Pb/^{206}Pb$ age value is shown in Fig. 4b. These data suggest that the crystallization age of the zircons is 2720 ± 8 Ma. Some zircon points yield younger but also concordant age values, up to 2690–2680 Ma, which could be caused by either the long-lasting crystallization of the zircons or the openness of their U–Pb isotopic system during a certain time after their crystallization. The closure temperature of the U–Pb isotopic system of zircon is higher than 800–900°C.

Our isotopic results provide reliable enough evidence of the Archean age of eclogites in the Gridino melange zone of the Belomorian Mobile Belt.

## GEOLOGICAL SETTING OF THE ROCKS AND THEIR PETROGRAPHY

The main petrologic characteristics of the genesis of the eclogites and the symplectitic rocks produced by their decompressional retrogression are discussed on the basis of studying the petrography of the rocks and their main rock-forming minerals with the use of numerous microprobe analyses. As of now, five locali-

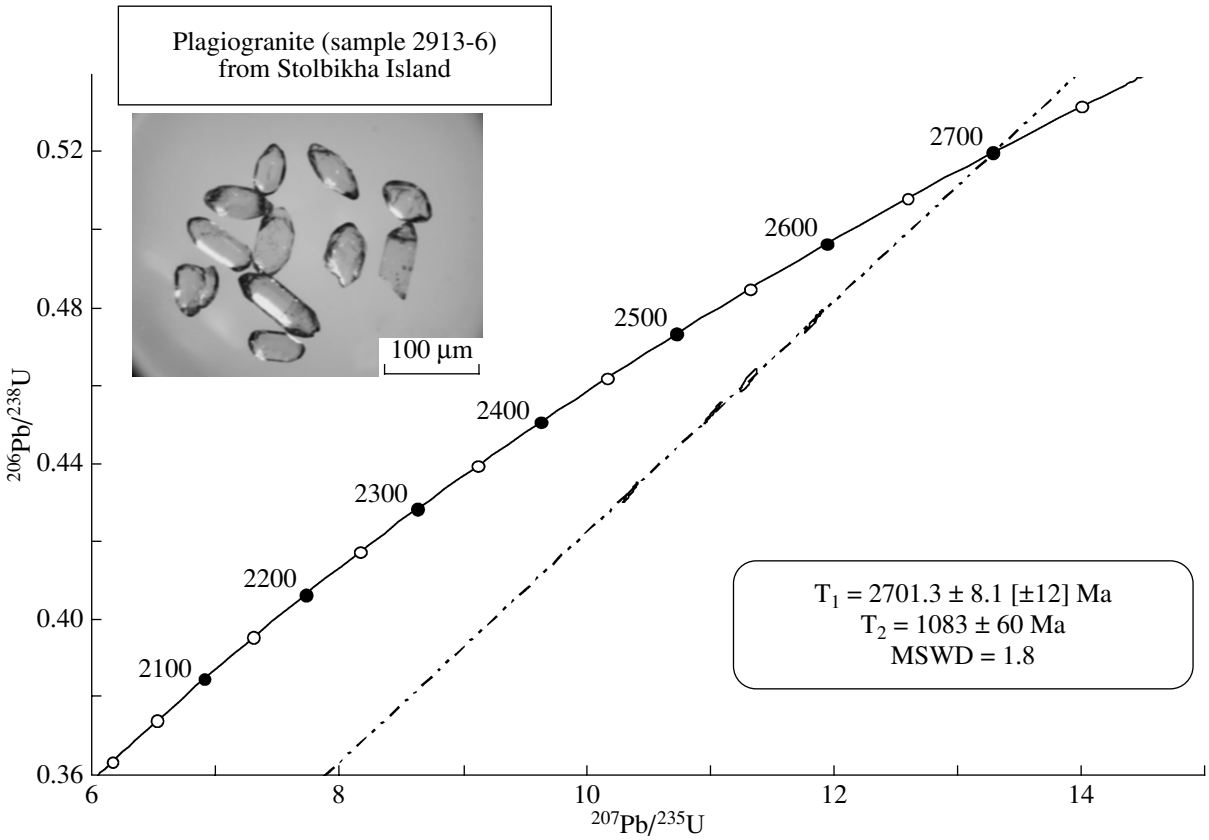


**Fig. 3.** Concordia diagram for zircons from plagiogranite (sample 2913-6) sampled at Stolbikha Island. The upper intercept of the discordia and concordia ($T_1$) corresponds to 2701.3 ± 8.1 Ma, the lower intercept corresponds to 1083 ± 60 Ma. The photograph shows zircons from the plagiogranite. The surfaces of the grains are slightly abraded. No analyzer.

ties of Archean eclogites were found in which rocks with variably preserved garnet–omphacite assemblages occur (Fig. 5).

### *Eclogite (Sample V-3 or Sample 2913-12) and Symplectitic Apoeclogites (Sample V-3-1 or Sample 2913-11 and Sample V-3-2)*

These rocks were among the first eclogites found on Stolbikha Island (Volodichev, 1977) (Fig. 2) as a 6 × 5 m eclogite fragment. The eastern part of this fragment consists of eclogite, and in its western part is banded symplectitic apoeclogite folded into isoclinal folds (samples V-3-1 or 2913-11 and V-3-2). The banding of the rock is accentuated by alternating layers of symplectitic apoeclogites and garnet amphibolites that developed after these rocks. All of these rock varieties are similar in chemical composition. They are cut by a pegmatite vein no more than 20 cm thick, with a clearly pronounced contact amphibolization zone. The geochronologic sample of the symplectitic apoeclogite (sample 2913-11) was taken from this exposure, and zircons from this sample yielded an Archean age of 2720 ± 8 Ma.

The host rock is amphibole and biotite (±*Grt*) gneiss-granite, which is cut by a steeply dipping vein of Archean (2701.3 ± 8.1 Ma) plagiogranite in the coastal exposures west of the fragment (Fig. 2).[2]

In spite of its significant overprinted transformations, only the eclogite of this sample contains preserved patches of bimineralic *Grt–Omp* composition and has an equigranular texture with homogeneous unzoned mineral grains, which are practically devoid of inclusions (Fig. 6). The omphacite in this rock contains ~30% of the *Jd* component on average (Table 3, analysis 2), with the *Jd* concentration varying relatively insignificantly (from 27 to 31%). The garnet is quite poor in pyrope (20–22% *Prp*) but is relatively rich in the Ca-component (28–31% *Grs*) (Table 3, analysis 1). A typical (and predominant) accessory mineral is rutile.

Rocks in these patches show traces of the initial stages of the overprinted processes that resulted in the

[2] Mineral symbols: *Alm*—almandine, *Am*—amphibole, *An*—anorthite, *Bt*—biotite, *Cpx*—clinopyroxene, *Di*—diopside, *Ed*—edenite, *Ed-Hbl*—edenitic hornblende, *Gln*—glaucophane, *Grt*—garnet, *Grs*—grossular, *Hbl*—hornblende, *Jd*—jadeite, *Ky*—kyanite, *Omp*—omphacite, *Pl*—plagioclase, *Prg*—pargasite, *Prg-Hbl*—parasitic hornblende, *Prp*—pyrope, *Qtz*—quartz, *Sil*—sillimanite, *Sps*—spessartine, *Ts*—tschermakite, *Uv*—uvarovite.

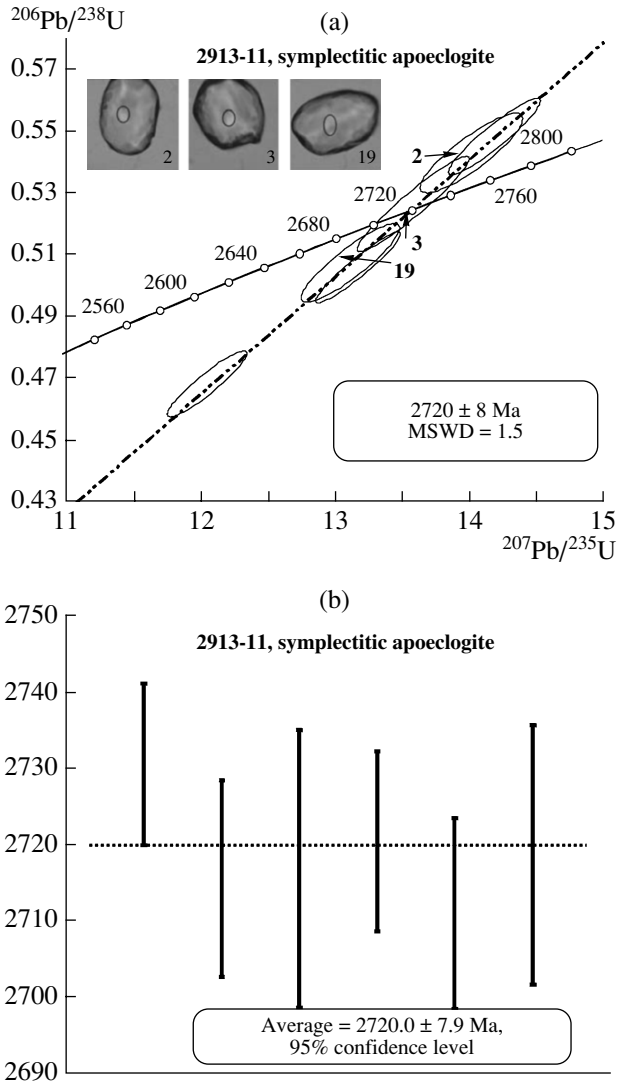


**Fig. 4.** (a) Concordia diagram and (b) histogram of age values obtained from the $^{207}Pb/^{206}Pb$ isotopic ratio for zircons from symplectitic apoeclogite (sample 2913-11) from Stolbikha Island (NORDSIM ion microprobe data). Inset: zircon grains from this sample. The morphology of these zircon crystals is similar to that of zircons from high-pressure granulites and eclogites. Circles correspond to the sites of spot analyses. The grains are +100 μm in size. No analyzer.

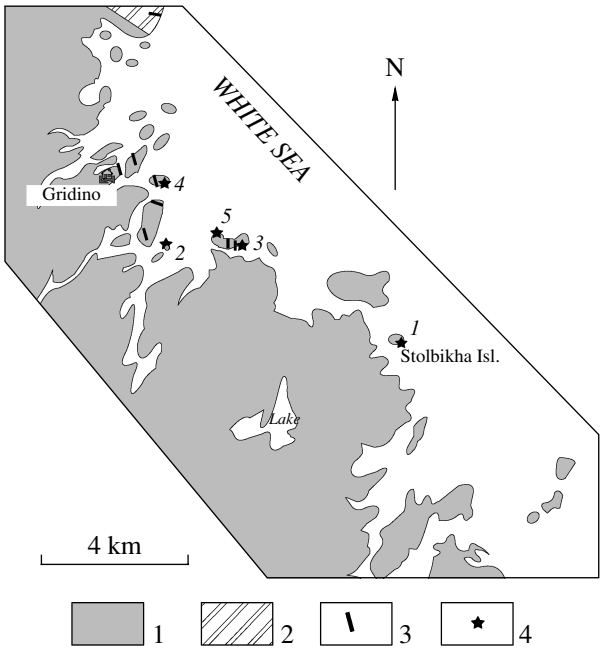


**Fig. 5.** Sampling sites of the Archean eclogites and symplectitic apoeclogites.

(1) Eclogite-bearing complex of extensively migmatized rocks of the tectonic melange zone; (2) tonalite-gneiss; (3) Early Proterozoic (~2.44 Ga) dikes of the lherzolite–gabbronorite complex; (4) sampling sites: 1—samples V-3 (2913-12), V-3-1 (2913-11), and V-3-2 (Stolbikha Island); (2) sample V-7-8 (small island southeast of Second Kokkov Island); (3) sample V-6-2 (Izbnaya Luda Island); (4) sample V-10-1 (Vorotnaya Luda Island); (5) sample V-7-2 (island northwest of Izbnaya Luda Island).

development of fine-grained plagioclase (22% *An*, Table 3, analysis 4) coupled with a decrease in the *Jd* concentration to 16% in the margins of omphacite grains (Table 3, analysis 3). The further development of the overprinted processes was responsible for the more extensive formation of $Pl_{25–26}$ and the crystallization of large $Grt^{18–20}_{30–31}$ porphyroblasts with inclusions of apatite, an ore mineral, quartz, and plagioclase.[3] Although $Omp_{28–30}$ grains are still preserved, *Cpx* and *Pl* symplectites appear, marking the transition to symplectitic apoeclogites, which compose patches in the rock. Later, amphibole (pargasitic hornblende) crystallizes in these patches in the form of individual large homogeneous sub- and euhedral crystals at contacts between garnet and *Cpx-Pl* symplectitic groundmass and in the latter (Fig. 7).

Samples V-3-1 or 2913-11 and V-3-2 were taken from different bands of the symplectitic apoeclogites deformed into isoclinal folds. The symplectitic apoeclogite of sample V-3-1 (2913-11) is noted for the occurrence of bytownite with 85% *An* (Table 3, analysis 5), which is, judging from petrographic data, a relic inherited from the magmatic protolith. The rock consists of clinopyroxene $Di_9$ in association with $Pl_{43–49}$, which compose symplectitic aggregates (Table 3, analyses 8, 9), and large, relatively homogeneous garnet grains $Grt^{22–24}_{28–32}$, whose composition in the margins corresponds to $Grt^{18–20}_{29–33}$ (Table 3, analyses 6, 7). This garnet population occurs in association with $Di_6$, which develops as finer-grained symplectite with $Pl_{38–42}$ (Table 3, analyses 10, 11). This composition of plagio-

[3] Subscript indices near *Omp* and *Di* symbols denote the *Jd* contents, and analogous indices near *Pl* correspond to its *An* contents; superscript and subscript indices near *Grt* denote its *Prp* and *Grs* contents, respectively.

**Table 2.** U–Pb isotopic data on zircons from symplectitic apoeclogite (sample 2913-11)

| Spot analysis | Concentration, ppm | | | Th/U | $^{206}Pb$, % | Isotopic ratios | | Isotopic age, Ma | Discordance, % |
|---|---|---|---|---|---|---|---|---|---|
| | U | Th | Pb | | | $^{206}Pb/^{238}U$ | $^{207}Pb/^{235}U$ | $^{207}Pb/^{206}Pb$ | |
| 1 | 58 | 26 | 39 | 0.45 | 0.00 | 0.5063 ± 93 | 13.170 ± 257 | 2731 ± 11 | –4 |
| 1b | 71 | 28 | 49 | 0.40 | 0.00 | 0.5268 ± 126 | 13.581 ± 343 | 2716 ± 13 | 1 |
| 2 | 24 | 13 | 17 | 0.53 | 0.00 | 0.5397 ± 107 | 13.685 ± 316 | 2688 ± 19 | 4 |
| 3 | 42 | 19 | 29 | 0.44 | 0.00 | 0.5247 ± 108 | 13.346 ± 297 | 2694 ± 14 | 1 |
| 4 | 77 | 20 | 61 | 0.26 | 0.64 | 0.6367 ± 155 | 15.899 ± 484 | 2663 ± 30 | 24 |
| 5 | 91 | 25 | 62 | 0.27 | 0.00 | 0.5392 ± 101 | 13.383 ± 271 | 2653 ± 13 | 6 |
| 5a | 35 | 12 | 25 | 0.33 | 0.00 | 0.5433 ± 105 | 14.016 ± 313 | 2717 ± 18 | 4 |
| 5b | 54 | 19 | 36 | 0.36 | 0.00 | 0.5157 ± 127 | 12.938 ± 337 | 2671 ± 14 | 0.5 |
| 6 | 66 | 22 | 46 | 0.33 | 0.00 | 0.5487 ± 101 | 14.186 ± 280 | 2721 ± 12 | 4 |
| 6b | 86 | 22 | 63 | 0.26 | 0.13 | 0.5796 ± 121 | 14.820 ± 328 | 2702 ± 12 | 11 |
| 7 | 68 | 38 | 48 | 0.56 | 0.36 | 0.5309 ± 98 | 13.273 ± 261 | 2665 ± 12 | 4 |
| 8 | 155 | 63 | 95 | 0.40 | 0.00 | 0.4685 ± 88 | 12.043 ± 243 | 2711 ± 12 | –10 |
| 15 | 44 | 20 | 29 | 0.45 | 0.00 | 0.5077 ± 104 | 13.112 ± 300 | 2719 ± 17 | –3 |
| 17 | 37 | 13 | 25 | 0.35 | 0.27 | 0.5138 ± 111 | 13.133 ± 310 | 2702 ± 16 | –1 |
| 18 | 92 | 27 | 58 | 0.29 | 0.00 | 0.4988 ± 101 | 12.733 ± 270 | 2700 ± 10 | –4 |
| 19 | 17 | 5 | 11 | 0.26 | 0.00 | 0.5024 ± 119 | 12.782 ± 363 | 2694 ± 25 | –3 |
| 20 | 31 | 11 | 20 | 0.36 | 0.00 | 0.5039 ± 111 | 12.769 ± 309 | 2687 ± 17 | –3 |
| 21 | 88 | 45 | 60 | 0.51 | 0.09 | 0.5114 ± 103 | 12.695 ± 265 | 2653 ± 9 | 0.4 |

clase is anomalous for symplectites in the symplectitic apoeclogites.

No such anomalies were noted in sample V-3-2, which is symplectitic apoeclogite typical of this area and containing coarse lamellar to globular symplectites of clinopyroxene $Di_8$ with plagioclase $Pl_{24}$ (Table 3, analyses 13, 14). Garnet occurs in this rock as larger compositionally homogeneous grains $Grt^{21–23}_{24–25}$ (Table 3, analysis 12). The rock pervasively contains amphibole: later crystals of edenitic hornblende (as in sample V-3) in the symplectitic *Cpx–Pl* groundmass, along with $Pl_{25}$ and quartz, at contacts of the groundmass with garnet grains (Table 3, analyses 15, 16). Amphibole was also found in the form of inclusions in garnet $Grt^{23}_{25}$.

### *Altered eclogite (Sample V-7-8)*

This sample was taken in the southwestern part of a small island southeast of Second Kokkov Island (Fig. 5), in which typical agmatites with relatively low amounts (no more than 25%) of vein material are exposed. The paleosome is strongly dominated by variably altered medium-grained symplectitic amphibolized apoeclogites with relics of relatively fine-grained less altered eclogites (which are represented by sample B-7-8).

Along with the principal minerals of the rock (garnet and clinopyroxene), it contains minor amounts of plagioclase and amphibole, quartz, and rare flakes of biotite; the accessory minerals are usually dominated by rutile. The texture of the rock is heteroblastic: the clinopyroxene–amphibole–plagioclase groundmass contains large garnet grains with abundant inclusions (mostly of quartz). The omphacite, which dominates among the clinopyroxenes, shows a well pronounced decompressional zoning (revealed by microprobe analyses) with an average composition of $Omp_{33}$ in the cores (Table 3) and 26–35% *Jd* (up to 40%, $Na_2O$ = 5.74 wt %, $Al_2O_3$ = 10.58 wt %) and $Omp_{21}$ in the margins. This process was associated with the development of chains of fine-grained $Pl_{17}$ aggregates in the interstices of clinopyroxene (Fig. 8), a process described by the reaction $Omp^{c}_{33} \longrightarrow Omp^{m}_{21} + Pl^{int}_{17}$ (Table 3, analyses 20–22). This process resulted in the disintegration of the protoomphacitic matrix of the rock with the development of a texture of concentric or semiconcentric domains of grains or granular aggregates of omphacitic clinopyroxene in the core, *Omp–Di* in the peripheries, and outermost discontinuous rims of plagioclase (produced by the reaction written above) in the form of aggregates of small grains that mark the boundaries of the domains (Fig. 8). The central parts of some domains consist of thin symplectitic *Cpx–Pl* intergrowths (Fig. 9), which seem to have developed after omphacite cores (which were the richest in jadeite) during further decompression. The symplectites consist of a single block or are mosaic and are made up of fragments with different patterns of mineral aggregates (Fig. 9), which

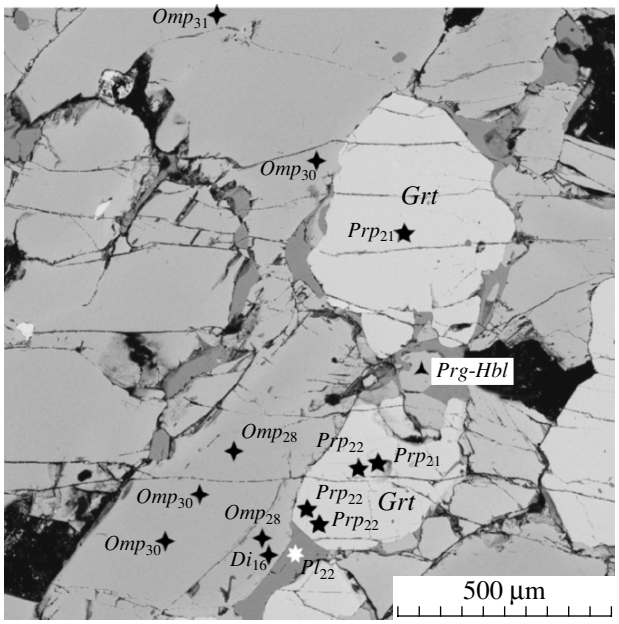


**Fig. 6.** Best preserved eclogite with homogeneous unzoned garnet and omphacite crystals. The weak secondary alterations are manifested in the form of newly formed *Pl* and *Di* in the thin marginal zone of *Omp* crystals and as newly formed *Pl* and *Prg-Hbl* at *Grt–Omp* contacts. Thin section V-3. Back-scattered image.

seem to replicate the shapes of grains of the precursor mineral. Clinopyroxene in the symplectite is *Di* with 12% *Jd*, plagioclase is oligoclase (25% *An*; Table 3, analyses 26, 27). The reaction rims are pronounced more clearly and are dominated by *Cpx* of transformed heterogeneous composition: *Di* with 18% *Jd* in some parts and *Di* with 8% *Jd* in others (Fig. 9, Table 3, analyses 28, 29), near which a part of the rim consists of edenite.

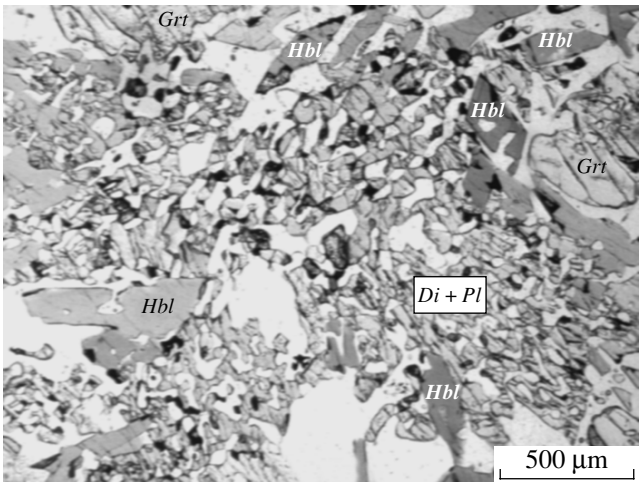


**Fig. 7.** Symplectitic apoeclogite with amphibole (mostly of *Prg–Hbl* composition), which is one of the youngest minerals that occurs as relatively large homogeneous subhedral and euhedral crystals at contacts of garnet with the symplectitic *Cpx–Pl* groundmass and in the latter. Thin section V-3a. No analyzer.

The garnet is also compositionally heterogeneous, but its zoning is less clear. One of the analyzed grains was more homogeneous chemically, with *Prp* variations from 26.5 to 28.2% (Table 3, analysis 17). Another grain was weakly zonal: 27% *Prp* in the core and 24.5% in the margin (Table 3, analyses 18, 19; Fig. 7). A third grain consisted mostly of $Grt^{24}$ with a part having the composition $Grt^{23}$ and containing inclusions of $Di_{15}$ and $Pl_{19}$ (Table 3, analyses 23–25).

The amphibole is pargasitic hornblende. The textural settings of this mineral and *Pl* (17% *An*) (Table 3, analyses 30, 31) in the rock are analogous to those in samples V-3 and V-3-2 (see above). One amphibole grain had a prograde zoning with $X_{Fe}$ decreasing and the pargasite content decreasing (Table 3, analyses 32, 33; Table 10). Edenite is spread much less widely and, as was mentioned above, occurs in association with diopside during the symplectitic stage of eclogite transformations.

### *Altered Eclogite (Sample V-6-2)*

This sample was taken at Izbnaya Luda Island (Fig. 5), southeast of the fisherman's lodge, within 8–10 m from the contact of an early Proterozoic gabbronorite dike. The geologic setting of this eclogite and its petrography are closer to those of the rock of sample V-7-8 (see above). The clinopyroxene has a well pronounced zoning: $Omp_{31} \longrightarrow Omp_{22} + Pl_{18}$ (Table 3, analyses 37–39). The garnet has the following retrograde zoning: $Grt_c^{28} \longrightarrow Grt_m^{27}$ or $Grt_c^{25}$ (Table 3, analyses 34, 36, 40). The core of $Grt^{28}$ contains inclusions of $Omp_{30}$, and $Grt^{25}$ bears inclusions of $Di_7$ and $Pl_{21}$ (Table 3, analyses 35, 40–42). These relations of mineral phases allowed us to determine more accurately the *Grt–Cpx* and *Grt–Cpx–Pl* mineral assemblages (Table 4).

The later amphibole in this eclogite is, as in sample V-7-8, Fe-rich pargasitic hornblende. The rock contains minor amounts of bright brown biotite ($TiO_2$ = 3.70 and

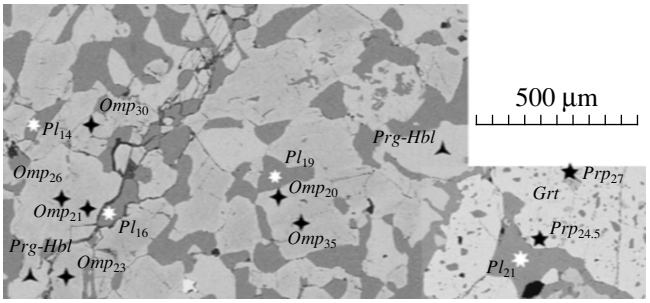


**Fig. 8.** Decompressional zoning in garnet and omphacite with newly formed interstitial plagioclase developing in the omphacite in the form of discontinuous chains of grains by the reaction $Omp_1 \longrightarrow Omp_2 + Pl$. "Slow" decompression stage. Thin section V-7-8. Back-scattered image.

**Table 3.** Chemical and normative compositions of minerals from Archean eclogites and symplectitic apoeclogites of the Belomorian Mobile Belt

| Component | sample V-3 | | | | sample V-3-1 | | | | | | |
|---|---|---|---|---|---|---|---|---|---|---|---|
| | 1[1] | 2 | 3 | 4 | 5 | 6 | 7 | 8 | 9 | 10 | 11 |
| | $Grt_{hom} - Omp_{hom}$ | | $Di_m - Pl$ | | $Pl_{rel}$ | $Grt_c - Grt_m$ | | $(Di + Pl)_s$ | | $(Di + Pl)_s$ | |
| | 7[2] | 11 | 1 | 2 | 3 | 6 | 2 | 4 | 4 | 3 | 2 |
| $SiO_2$ | 37.62 | 52.08 | 51.59 | 60.73 | 47.24 | 38.93 | 38.46 | 50.31 | 56.63 | 51.84 | 57.81 |
| $TiO_2$ | 0.09 | 0.17 | 0.25 | 0.06 | 0.01 | 0.09 | – | 0.34 | – | 0.37 | 0.08 |
| $Al_2O_3$ | 21.31 | 6.99 | 5.38 | 23.17 | 33.53 | 20.94 | 20.99 | 6.26 | 27.25 | 3.35 | 26.14 |
| $Cr_2O_3$ | n.a. | n.a. | 0.27 | n.a. | 0.06 | 0.08 | 0.35 | 0.15 | 0.08 | 0.26 | 0.05 |
| FeO* | 21.83 | 5.28 | 7.34 | 0.20 | 0.07 | 22.19 | 23.70 | 7.91 | 0.10 | 7.64 | 0.26 |
| MnO | 0.80 | 0.06 | 0.08 | 0.11 | – | 0.56 | 0.63 | 0.07 | 0.01 | 0.14 | 0.02 |
| MgO | 5.75 | 10.80 | 12.10 | – | – | 6.14 | 4.64 | 11.70 | – | 13.03 | – |
| CaO | 10.43 | 17.16 | 20.71 | 4.86 | 17.41 | 11.03 | 11.27 | 21.99 | 9.73 | 22.48 | 8.59 |
| $Na_2O$ | 0.08 | 4.17 | 2.24 | 9.30 | 1.64 | – | – | 1.25 | 6.12 | 0.84 | 6.95 |
| $K_2O$ | – | – | – | – | 0.04 | 0.03 | – | 0.02 | 0.10 | 0.05 | 0.14 |
| Total | 97.91 | 96.71 | 99.96 | 98.43 | 100.00 | 99.99 | 100.04 | 100.00 | 100.02 | 100.00 | 100.04 |
| *Prp* | 22.3 | | | | | 23.0 | 17.6 | | | | |
| *Alm* | 47.2 | | | | | 46.3 | 50.4 | | | | |
| *Sps* | 1.6 | | | | | 1.3 | 1.3 | | | | |
| *Grs* | 28.9 | | | | | 29.3 | 30.2 | | | | |
| *Uv* | – | | | | | 0.1 | 0.5 | | | | |
| *F* | 67.9 | 21.5 | 25.4 | | | 66.8 | 74.0 | 27.5 | | 24.7 | |
| *An*, % | | | | 22.4 | 85.2 | | | | 46.5 | | 40.3 |
| *Jd*, % | | 30.1 | 15.9 | | | | | 9.1 | | 6.3 | |

| Component | sample V-3-2 | | | | | sample V-7-8 | | | | | |
|---|---|---|---|---|---|---|---|---|---|---|---|
| | 12 | 13 | 14 | 15 | 16 | 17 | 18 | 19 | 20 | 21 | 22 |
| | $Grt_{hom}$ | $(Di + Pl)_s$ | | $Ed - Hbl - Pl$ | | $Grt_{hom}$ | $Grt_c - Grt_m$ | | $Omp_c \longrightarrow Omp_m + Pl_{int}$ | | |
| | 3 | 3 | 4 | 4 | 2 | 5 | 2 | 1 | 4 | 3 | 2 |
| $SiO_2$ | 38.75 | 52.00 | 62.68 | 44.12 | 62.29 | 39.00 | 39.31 | 38.55 | 52.34 | 51.78 | 64.93 |
| $TiO_2$ | 0.05 | 0.21 | 0.02 | 1.68 | 0.03 | 0.09 | 0.03 | 0.22 | 0.13 | 0.24 | – |
| $Al_2O_3$ | 21.21 | 2.91 | 23.58 | 11.05 | 23.71 | 21.45 | 21.58 | 21.45 | 9.88 | 7.17 | 22.16 |
| $Cr_2O_3$ | 0.06 | 0.08 | 0.04 | 0.12 | 0.07 | 0.05 | – | 0.07 | 0.09 | 0.12 | 0.02 |
| FeO* | 24.87 | 8.52 | 0.12 | 14.08 | 0.09 | 23.30 | 23.17 | 24.64 | 6.83 | 7.42 | 0.10 |
| MnO | 0.85 | 0.18 | – | 0.06 | – | 0.58 | 0.61 | 0.83 | 0.04 | 0.04 | 0.08 |
| MgO | 5.99 | 13.01 | – | 12.32 | – | 7.21 | 7.22 | 6.61 | 9.63 | 11.14 | – |
| CaO | 9.11 | 21.54 | 5.22 | 11.27 | 5.35 | 8.36 | 8.66 | 8.42 | 15.77 | 18.58 | 3.70 |
| $Na_2O$ | – | 1.11 | 8.87 | 1.88 | 8.81 | – | – | – | 4.65 | 2.95 | 9.93 |
| $K_2O$ | 0.02 | – | 0.35 | 1.02 | 0.34 | 0.04 | – | 0.01 | 0.03 | 0.03 | 0.26 |
| Total | 100.91 | 99.56 | 100.88 | 97.60 | 100.69 | 100.08 | 100.58 | 100.80 | 99.39 | 99.47 | 101.18 |
| *Prp* | 22.2 | | | | | 27.1 | 26.9 | 24.7 | | | |
| *Alm* | 51.7 | | | | | 49.1 | 48.5 | 51.3 | | | |
| *Sps* | 1.9 | | | | | 1.3 | 1.3 | 1.6 | | | |
| *Grs* | 24.1 | | | | | 22.5 | 23.3 | 22.3 | | | |
| *Uv* | 0.1 | | | | | – | – | 0.1 | | | |
| *F* | 70.0 | 26.9 | | 39.1 | | 64.4 | 64.4 | 67.5 | 28.5 | 27.2 | |
| *An*, % | | | 24.1 | | 24.7 | | | | | | 16.8 |
| *Jd*, % | | 8.0 | | | | | | | 32.9 | 21.1 | |

**Table 3.** (Contd.)

| Component | sample V-7-8 | | | | | | | | | | |
|---|---|---|---|---|---|---|---|---|---|---|---|
| | 23 | 24 | 25 | 26 | 27 | 28 | 29 | 30 | 31 | 32 | 33 |
| | $Grt_{host} - Di_{incl} - Pl_{incl}$ | | | $(Di + Pl)_s$ | | $Di_{rim}$ | $Di_{rim}$ | *Prg-Hbl – Pl* | | $Prg\text{-}Hbl_c \longrightarrow Prg\text{-}Hbl_m$ | |
| | 2 | 1 | 1 | 3 | 2 | 1 | 1 | 5 | 2 | 1 | 1 |
| $SiO_2$ | 38.53 | 52.65 | 62.52 | 53.04 | 62.20 | 53.82 | 53.77 | 42.68 | 64.34 | 42.05 | 41.86 |
| $TiO_2$ | 0.02 | 0.13 | – | 0.34 | – | 0.33 | 0.24 | 1.01 | 0.03 | 0.99 | 0.79 |
| $Al_2O_3$ | 21.21 | 3.40 | 22.20 | 3.80 | 22.92 | 3.38 | 7.05 | 12.66 | 21.92 | 13.07 | 14.21 |
| $Cr_2O_3$ | 0.07 | 0.04 | 0.10 | 0.06 | 0.08 | 0.02 | 0.04 | 0.07 | 0.05 | – | 0.06 |
| FeO* | 24.62 | 8.30 | 0.37 | 6.58 | 0.30 | 7.29 | 6.61 | 13.59 | 0.22 | 14.03 | 13.32 |
| MnO | 0.81 | 0.06 | – | 0.06 | 0.04 | 0.08 | 0.26 | 0.06 | – | 0.13 | – |
| MgO | 6.33 | 12.61 | – | 12.87 | – | 12.08 | 9.91 | 12.70 | – | 12.31 | 12.54 |
| CaO | 8.48 | 19.22 | 4.08 | 20.67 | 4.90 | 21.88 | 19.74 | 10.82 | 3.68 | 10.90 | 10.78 |
| $Na_2O$ | – | 2.08 | 9.30 | 1.61 | 9.05 | 1.12 | 2.39 | 2.66 | 9.71 | 2.83 | 2.71 |
| $K_2O$ | 0.05 | 0.04 | 0.11 | 0.01 | 0.25 | – | – | 0.82 | 0.19 | 0.88 | 0.79 |
| Total | 100.12 | 98.53 | 98.68 | 99.04 | 99.74 | 100.00 | 100.01 | 97.07 | 100.14 | 97.19 | 97.06 |
| *Prp* | 23.8 | | | | | | | | | | |
| *Alm* | 51.8 | | | | | | | | | | |
| *Sps* | 1.6 | | | | | | | | | | |
| *Grs* | 22.7 | | | | | | | | | | |
| *Uv* | 0.1 | | | | | | | | | | |
| *F* | 68.5 | 27.0 | | 22.4 | | 25.3 | 27.2 | 37.5 | | 39.0 | 37.3 |
| *An*, % | | | 19.4 | | 22.7 | | | | 17.1 | | |
| *Jd*, % | | 15.0 | | 11.6 | | 8.2 | 17.6 | | | | |

| Component | sample V-6-2 | | | | | | | | | | |
|---|---|---|---|---|---|---|---|---|---|---|---|
| | 34 | 35 | 36 | 37 | 38 | 39 | 40 | 41 | 42 | 43 | 44 |
| | $(Grt_c - Omp_{inc}) - Grt_m$ | | | $Omp_c \longrightarrow Omp_m + Pl_{int}$ | | | $Grt_{host} - Di_{inc} - Pl_{inc}$ | | | *Prg-Hbl – Pl* | |
| | 3 | 3 | 1 | 4 | 2 | 3 | 2 | 1 | 1 | 2 | 1 |
| $SiO_2$ | 38.78 | 53.43 | 38.45 | 52.99 | 52.12 | 63.49 | 38.59 | 53.47 | 62.60 | 42.81 | 62.80 |
| $TiO_2$ | 0.12 | 0.28 | 0.18 | 0.30 | 0.25 | 0.03 | 0.03 | 0.12 | – | 0.75 | 0.01 |
| $Al_2O_3$ | 21.29 | 8.82 | 21.33 | 9.07 | 7.85 | 22.41 | 21.23 | 1.55 | 22.73 | 13.59 | 23.04 |
| $Cr_2O_3$ | 0.09 | 0.19 | 0.03 | 0.10 | 0.10 | 0.01 | 0.06 | 0.07 | – | 0.10 | 0.11 |
| FeO* | 22.96 | 5.42 | 24.13 | 6.54 | 7.04 | 0.15 | 24.10 | 7.95 | 0.35 | 12.80 | 0.18 |
| MnO | 0.93 | 0.06 | 0.74 | 0.05 | 0.13 | 0.04 | 1.10 | 0.20 | 0.10 | 0.05 | 0.08 |
| MgO | 7.64 | 10.50 | 7.13 | 9.80 | 11.00 | – | 6.68 | 14.13 | – | 13.13 | – |
| CaO | 8.14 | 16.95 | 8.01 | 16.71 | 18.89 | 3.92 | 8.20 | 21.31 | 4.63 | 11.16 | 4.45 |
| $Na_2O$ | – | 4.31 | – | 4.41 | 3.10 | 9.64 | – | 1.12 | 9.31 | 2.41 | 9.02 |
| $K_2O$ | 0.04 | 0.05 | – | 0.03 | – | 0.30 | – | 0.07 | 0.27 | 1.23 | 0.32 |
| Total | 99.99 | 100.01 | 100.00 | 100.00 | 100.48 | 99.99 | 99.99 | 99.99 | 99.99 | 98.03 | 100.01 |
| *Prp* | 28.3 | | 26.6 | | | | 25.0 | | | | |
| *Alm* | 47.9 | | 50.4 | | | | 50.6 | | | | |
| *Sps* | 2.0 | | 1.6 | | | | 2.4 | | | | |
| *Grs* | 21.7 | | 21.4 | | | | 22.0 | | | | |
| *Uv* | 0.1 | | – | | | | – | | | | |
| *F* | 62.8 | 22.5 | 65.5 | 27.2 | 26.5 | | 67.0 | 24.0 | | 35.4 | |
| *An*, % | | | | | | 18.0 | | | 21.2 | | 21.0 |
| *Jd*, % | | 30.3 | | 31.4 | 22.0 | | | 6.7 | | | |

**Table 3.** (Contd.)

| Component | sample V-6-2 | | sample V-10-1 | | | | | | | | |
|---|---|---|---|---|---|---|---|---|---|---|---|
| | 45 | 46 | 47 | 48 | 49 | 50 | 51 | 52 | 53 | 54 | 55 |
| | $(Bt + Pl)_s$ | | $Grt_c - Grt_{imd} - Grt_{m'}$ | | | $Grt_c - Grt_m$ | | $Omp_c - Di_m$ | | $(Di + Pl)_s$ | |
| | 2 | 1 | 1 | 2 | 1 | 3 | 1 | 2 | 1 | 2 | 1 |
| $SiO_2$ | 37.27 | 63.02 | 38.67 | 38.57 | 37.75 | 38.69 | 38.19 | 54.89 | 52.89 | 53.29 | 64.16 |
| $TiO_2$ | 4.25 | – | 0.09 | 0.12 | 0.07 | 0.06 | 0.02 | 0.09 | 0.16 | 0.03 | – |
| $Al_2O_3$ | 13.86 | 22.64 | 21.65 | 21.88 | 21.40 | 21.93 | 21.88 | 6.74 | 5.83 | 4.06 | 22.29 |
| $Cr_2O_3$ | 0.18 | – | n.a. | n.a. | n.a. | n.a. | n.a. | n.a. | n.a. | n.a. | n.a. |
| FeO* | 14.18 | 0.27 | 21.64 | 23.36 | 25.51 | 22.16 | 24.04 | 5.21 | 6.57 | 6.68 | 0.37 |
| MnO | – | – | 1.17 | 1.17 | 1.97 | 0.97 | 1.76 | 0.06 | 0.14 | 0.20 | 0.04 |
| MgO | 15.50 | – | 7.21 | 6.35 | 5.53 | 7.29 | 6.18 | 11.33 | 12.06 | 12.94 | – |
| CaO | – | 4.28 | 9.36 | 8.52 | 7.70 | 8.72 | 7.90 | 17.30 | 19.65 | 21.00 | 3.51 |
| $Na_2O$ | 0.27 | 9.41 | 0.16 | – | – | 0.12 | – | 4.37 | 2.65 | 1.79 | 9.40 |
| $K_2O$ | 9.50 | 0.37 | 0.02 | – | 0.07 | 0.02 | 0.04 | – | 0.03 | 0.01 | 0.22 |
| Total | 95.01 | 99.99 | 99.97 | 99.97 | 100.00 | 99.96 | 100.01 | 99.99 | 99.98 | 100.00 | 99.99 |
| *Prp* | | | 27.0 | 24.2 | 20.8 | 27.4 | 23.4 | | | | |
| *Alm* | | | 45.3 | 49.8 | 54.2 | 46.8 | 51.1 | | | | |
| *Sps* | | | 2.6 | 2.6 | 4.2 | 2.0 | 3.9 | | | | |
| *Grs* | | | 25.1 | 23.4 | 20.8 | 23.8 | 21.6 | | | | |
| *Uv* | | | – | – | – | – | – | | | | |
| *F* | 34.0 | | 62.6 | 67.4 | 72.2 | 63.1 | 68.7 | 20.5 | 23.4 | 22.5 | |
| *An*, % | | 19.7 | | | | | | | | | 16.9 |
| *Jd*, % | | | | | | | | 28.6 | 18.9 | 12.8 | |

| Component | sample V-10-1 | | | | | | | | | | | |
|---|---|---|---|---|---|---|---|---|---|---|---|---|
| | 56 | 57 | 58 | 59 | 60 | 61 | 62 | 63 | 64 | 65 | 66 | 67 |
| | $Omp_c \longrightarrow (Di_m + Pl)_s$ | | $Di_s$ | $(Di + Ed + Pl)_s$ | | | | $Prg$ | *Ed-Hbl* | *Ed* | $Ed_c \longrightarrow Ed\text{-}Hbl_m$ | |
| | 2 | 1 | 1 | 1 | 1 | 1 | 1 | 1 | 1 | 3 | 1 | 1 |
| $SiO_2$ | 55.12 | 53.01 | 64.12 | 53.30 | 53.57 | 48.75 | 63.44 | 43.20 | 45.74 | 49.34 | 50.10 | 45.74 |
| $TiO_2$ | 0.03 | 0.07 | 0.02 | 0.04 | 0.29 | 0.72 | – | 0.36 | 0.30 | 0.40 | 0.21 | 0.30 |
| $Al_2O_3$ | 6.74 | 3.94 | 22.59 | 1.34 | 2.84 | 8.76 | 22.61 | 15.07 | 12.15 | 8.49 | 8.29 | 12.15 |
| $Cr_2O_3$ | n.a. | n.a. | n.a. | n.a. | n.a. | n.a. | n.a. | n.a. | n.a. | n.a. | n.a. | n.a. |
| FeO* | 5.06 | 7.57 | 0.21 | 6.35 | 7.80 | 12.52 | 0.05 | 12.78 | 12.47 | 11.86 | 11.56 | 12.47 |
| MnO | 0.05 | 0.11 | – | 0.26 | 0.23 | 0.19 | 0.02 | 0.19 | 0.02 | 0.18 | 0.08 | 0.02 |
| MgO | 11.22 | 12.54 | 0.04 | 14.39 | 14.81 | 14.71 | – | 12.78 | 14.30 | 15.83 | 16.21 | 14.30 |
| CaO | 17.68 | 20.96 | 3.72 | 23.30 | 19.37 | 12.23 | 4.15 | 11.66 | 11.70 | 11.53 | 11.21 | 11.70 |
| $Na_2O$ | 4.06 | 1.68 | 9.04 | 0.92 | 0.93 | 1.47 | 9.46 | 2.55 | 2.42 | 1.72 | 1.75 | 2.42 |
| $K_2O$ | 0.03 | 0.10 | 0.25 | 0.08 | 0.12 | 0.60 | 0.24 | 1.41 | 0.85 | 0.60 | 0.55 | 0.85 |
| Total | 99.99 | 99.98 | 99.99 | 99.98 | 99.96 | 99.95 | 99.97 | 100.00 | 99.95 | 99.95 | 99.96 | 99.95 |
| *Prp* | | | | | | | | | | | | |
| *Alm* | | | | | | | | | | | | |
| *Sps* | | | | | | | | | | | | |
| *Grs* | | | | | | | | | | | | |
| *Uv* | | | | | | | | | | | | |
| *F* | 20.2 | 25.3 | | 19.8 | 22.8 | 32.3 | | 35.9 | 32.8 | 29.6 | 28.6 | 32.8 |
| *An*, % | | | 18.3 | | | | 19.2 | | | | | |
| *Jd*, % | 28.2 | 12.5 | | 5.8 | 7.2 | | | | | | | |

**Table 3.** (Contd.)

| Component | sample V-7-2 | | | | | | | | |
|---|---|---|---|---|---|---|---|---|---|
| | 68 | 69 | 70 | 71 | 72 | 73 | 74 | 75 | 76 |
| | $Grt_{hom}$ | $Omp_c - Di_m$ | | $(Di_c + Pl)_s - Di_m$ | | | *Prg-Hbl – Pl* | | *Ed-Hbl* |
| | 2 | 2 | 1 | 1 | 1 | 1 | 1 | 2 | 1 |
| $SiO_2$ | 39.82 | 51.70 | 53.42 | 50.80 | 64.53 | 52.72 | 43.98 | 64.54 | 46.38 |
| $TiO_2$ | 0.07 | 0.22 | 0.20 | 0.82 | 0.08 | 0.24 | 1.22 | 0.07 | 1.05 |
| $Al_2O_3$ | 21.64 | 8.47 | 2.66 | 5.23 | 23.00 | 6.09 | 12.48 | 23.34 | 10.30 |
| $Cr_2O_3$ | 0.09 | 0.03 | 0.09 | 0.11 | 0.04 | – | 0.12 | – | 0.07 |
| FeO* | 22.57 | 6.69 | 7.35 | 8.77 | 0.21 | 7.49 | 13.15 | 0.09 | 12.11 |
| MnO | 0.79 | 0.20 | – | 0.12 | 0.06 | 0.11 | – | – | 0.13 |
| MgO | 8.14 | 11.14 | 14.39 | 13.85 | – | 12.38 | 13.49 | – | 14.53 |
| CaO | 8.47 | 19.12 | 21.45 | 19.41 | 4.27 | 20.21 | 11.37 | 4.42 | 11.54 |
| $Na_2O$ | – | 3.18 | 1.18 | 1.38 | 9.45 | 2.32 | 2.35 | 9.70 | 1.88 |
| $K_2O$ | 0.02 | – | 0.11 | 0.26 | 0.40 | 0.07 | 1.24 | 0.25 | 0.75 |
| Total | 101.61 | 100.75 | 100.85 | 100.75 | 102.04 | 101.63 | 99.40 | 102.41 | 98.74 |
| *Prp* | 29.7 | | | | | | | | |
| *Alm* | 46.4 | | | | | | | | |
| *Sps* | 1.6 | | | | | | | | |
| *Grs* | 22.2 | | | | | | | | |
| *Uv* | 0.1 | | | | | | | | |
| *F* | 60.9 | 25.2 | 22.3 | 26.2 | | 25.3 | 35.4 | | 31.9 |
| *An*, % | | | | | 19.5 | | | 20.1 | |
| *Jd*, % | | 22.3 | 8.8 | 11.0 | | 16.5 | | | |

Note: Minerals were analyzed on a Camebax X-ray microprobe equipped with a Link AN 10 000 analytical set at the Institute of Experimental Mineralogy, Russian Academy of Sciences, and on electron microscopes: CamScan MV2300 (at the Institute of Experimental Mineralogy, Russian Academy of Sciences) and CamScan 4DV equipped with a Link AN 10 000 analytical set (Department of Petrography, Moscow State University; sample V-10-1). FeO*—all Fe determined as FeO, $F = Fe/(Fe + Mg) \times 100$, %; $An = Ca/(Ca + Na + K) \times 100$. The pyroxene nomenclature is according to (Marimoto, 1988), and amphibole nomenclature corresponds to (Leake, 1978); *% Jd* in *Cpx* was calculated in compliance with (Cawthorn and Collerson, 1974) using the PX computer program (Cebria, 1990). Abbreviations: **hom**—homogeneous, **c**—grain core, **imd**—intermediate zone of the grain, **m**—grain margin, **m'**—grain margins if the crystals have different zoning patterns in a single rock, **host**—host mineral, **incl**—mineral inclusion, **r**—reaction rim, **s**—symplectitic aggregate, **int**—interstitial, **rel**—relic mineral. [1]—Analysis number; [2]—number of analyses in the group for averaged compositions.

4.75 wt %), which occurs as separate flakes or in symplectitic aggregates with $Pl_{20}$ (Table 3, analyses 45, 46).

### *Eclogite (Sample V-10-1)*

Eclogites were found on Vorotnaya Island (Fig. 5) in a fragment of pyroxenite with traces of eclogitization. Unlike the rocks described above, this eclogite is a medium-grained rock with a pale green amphibole–clinopyroxene groundmass with rare larger porphyroblastic and poikiloblastic garnet crystals.

Retrograde zoning in this rock is clearly pronounced in the clinopyroxene: $Omp_{29} \longrightarrow Di_{19} \longrightarrow Di_{13} + Pl_{17}$ (Table 3, analyses 52–55) or $Omp_{28} \longrightarrow Di_{13} + Pl_{18}$ (Table 3, analyses 56–58) with clear symplectitic textures with $Di_{12–14}$ (Fig. 11). The garnet is also zonal: $Grt^{27} \longrightarrow Grt^{24} \longrightarrow Grt^{21}$ or $Grt^{27–28} \longrightarrow Grt^{23–24}$ (Table 3, analyses 47–51). The finer grained symplectites bear $Di_7$, $Pl_{19}$, and edenite. The abundant amphibole is Fe-rich pargasite, edenitic hornblende, and edenite. One amphibole grain was zonal: $Ed_c$ – $Ed\text{-}Hbl_m$ (Table 3, analyses 66, 67, Fig. 10), in compliance with the following sequence of amphibole formation (typical of all of the rocks): *Ed* ⟶ *Ed-Hbl* ⟶ *Prg-Hbl*. The rocks also contains 3–4% brown biotite.

### *Symplectitic Apoeclogite (Sample V-7-2)*

This rock was sampled on the shore of a nameless island, the first island north of Izbnaya Luda Island (Fig. 5). In this island, eclogites occur as the paleosome of migmatites, which is exposed at two localities

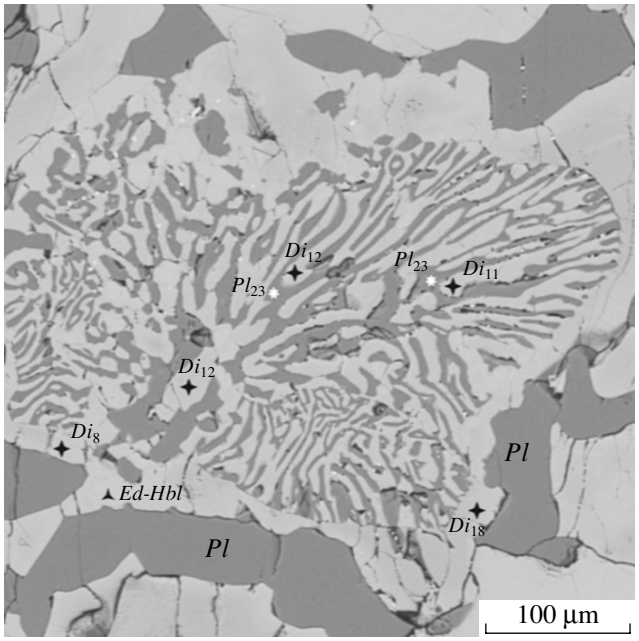


**Fig. 9.** Thin *Cpx–Pl* symplectitic aggregates developing in the central part of a decompresional microtexture of stage I (see Fig. 8) after an aggregate of omphacite grains, whose original contours corresponds to boundaries between domains with different textural patterns of mineral aggregates. The rim pronounced more clearly has a heterogeneous modified composition. Stage II of decompression. Thin section V-7-8. Back-scattered image.

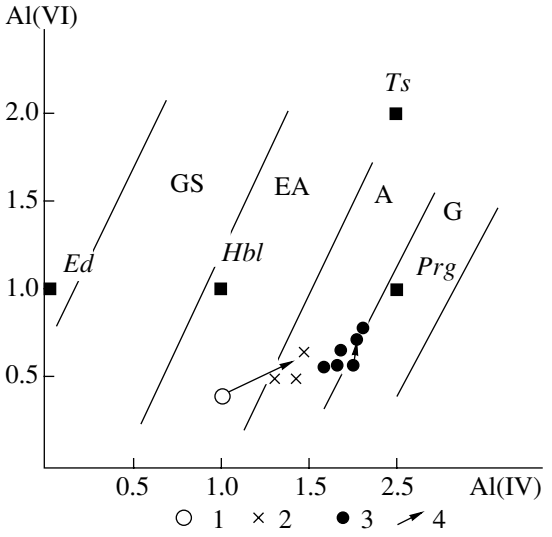


**Fig. 10.** Composition of Ca-amphiboles from the Archean eclogites and symplectitic apoeclogites.
(1) Edenite; (2) edenitic hornblende; (3) pargasite and pargasitic hornblende; (4) compositional trend in zonal amphibole grains from their cores to rims. The amphibole nomenclature is according to (Leake, 1978). The fields of metamorphic facies are given after (Mattana and Edgar, 1969): GS—greenschist, EA—epidote-amphibolite, A—amphibolite, G—granulite.

15 × 15 m each. The exposures are separated by a plagiogranite vein up to 10 m thick. West of it, the gneiss-granite vein material of the migmatite contains a large fragment of anchimonomineralic zoisite rock. The zoisite is white or, in places, pistachio green.

The geologic setting, textures, and compositions of the rocks are analogous to those in the exposures where samples V-7-8 and V-6-2 were taken. It is highly probable that some parts of this fragment contain relics of the primary eclogite (they will, perhaps, be identified in the course of the further examination of the rock), but as of now only clinopyroxene of the composition $Omp_{22}$ was found, whose symplectitic margins have the composition $Di_9$ and occur in association with $Pl_{21}$ (Table 3, analyses 69, 70). Another analyzed grain has a prograde (?) zoning (Fig. 12), with a core consisting of a coarse-grained symplectite of $Di_{11}$ and $Pl_{20}$ and a margin consisting of *Di* with 16% *Jd* (Table 3, analyses 71–73). These relations closely resemble those in the portions of sample V-7-8 containing fine-grained *Cpx–Pl* symplectites (Fig. 9). At the same time, this can be a relic of the prograde stage of the eclogitization process, similar to that documented by Korikovsky *et al.* (1997) in plagioclase-bearing eclogite-amphibolite of the Buchim block of the Serbo-Macedonian Massif in Macedonia. The homogeneous garnet of this rock is the richest in pyrope among garnets from the rocks of this group (30% *Prp*, 22% *Grs*; Table 3, analysis 68). The younger amphibole, which is Fe-rich pargasitic hornblende occurring in association with $Pl_{20}$ and edenitic hornblende (Table 3, analyses 74–76), develops at boundaries between garnet grains and *Cpx–Pl* symplectites.

## METAMORPHIC *P–T* PARAMETERS AND TRAJECTORIES

The equilibrium and reaction textures of the eclogites, the zoning of mineral grains, and inclusions in them can be used to calculate the *P–T* parameters of the eclogite metamorphism and its prograde and retrograde evolutionary paths.

The most informative indicator of metamorphic conditions is the *Jd* concentration in the clinopyroxene (Tables 3, 4, Fig. 12). Our samples contain four major groups of clinopyroxenes with jadeite contents gradually decreasing from the prograde metamorphic stage (*Omp* with 28–33 to 40% *Jd*, homogeneous crystals and the cores of grains) to the stages of the decompressional transformations (*Di–Omp* with 18–22% *Jd*, decompressional rims in association with interstitial *Pl*; *Di* with 9–13% *Jd* and with 6–8% *Jd*, symplectites with *Pl*).

The garnets in the eclogites are almost homogeneous, with *Prp* contents of 22–30% (Fig. 13). The variations in the *Prp* and *Grs* concentrations (22–30%) in individual samples were most probably controlled by the bulk chemistry of the rocks, particularly their Ca : Mg : Fe proportions. In this context, a noteworthy example is garnet in the eclogite of sample V-3 with a

**Table 4.** Metamorphic *P–T* parameters of the eclogites and symplectitic apoeclogites

| Sample | Mineral assemblage | | | | *T*, °C | | | | *P*, kbar | | | |
|---|---|---|---|---|---|---|---|---|---|---|---|---|
| | $Grt_{Prp}$ | $Cpx_{Jd}$ | $Pl_{An}$ | *Am* | *Grt–Cpx* | | *Hbl–Pl–Qtz* | *Grt–Hbl* | *Jd* isopleths | *Grt–Cpx–Pl–Qtz* | | *Hbl* |
| | | | | | (1) | (2) | (3) | (4) | (5) | (6) | (7) | (8) |
| V-3 | $Grt_{22}^{hom}$ | $Omp_{31}^{hom}$ | | | 740 | 660 | | | 14.2 | | | |
| V-3-1 | $Grt_{23}^{c}$ | $Di_{9}^{s}$ | $Pl_{47}^{s}$ | | 850 | 780 | | | 11.4 | 10.5 | 12.6 | |
| | $Grt_{18}^{m}$ | $Di_{6}^{s}$ | $Pl_{40}^{s}$ | | 710 | 640 | | | | 8.5 | 10.4 | |
| V-3-2 | $Grt_{22}^{hom}$ | $Di_{8}^{s}$ | $Pl_{24}^{s}$ | | 750 | 675 | | | | 10.4 | 12.2 | |
| | $Grt_{22}^{m}$ | | $Pl_{25}$ | *Ed-Hbl* | | | 670 | 630 | | | | 6.5 |
| V-7-8 | $Grt_{27}^{hom}$ | $Omp_{40}^{c}$ | | | 865 | 785 | | | 17.5 | | | |
| | $Grt_{27}^{c}$ | $Omp_{33}^{c}$ | | | 860 | 800 | | | 16.8 | | | |
| | $Grt_{25}^{m}$ | $Omp_{21}^{m}$ | $Pl_{17}^{int}$ | | 770 | 700 | | | 13.2 | 13.2 | 15.3 | |
| | $Grt_{24}^{host}$ | $Di_{15}^{inc}$ | $Pl_{19}^{inc}$ | | 765 | 690 | | | 12.0 | 12.0 | 14.5 | |
| | $Grt_{25}^{m}$ | | $Pl_{17}$ | *Prg-Hbl* | | | 715 | 650 | | | | 7.6 |
| V-6-2 | $Grt_{28}^{c}$ | $Omp_{30}^{c+inc}$ | | | 805 | 725 | | | 15.0 | | | |
| | $Grt_{27}^{m}$ | $Omp_{22}^{m}$ | $Pl_{18}^{int}$ | | 780 | 710 | | | 13.5 | 13.4 | 16.0 | |
| | $Grt_{25}^{host}$ | $Di_{7}^{inc}$ | $Pl_{21}^{inc}$ | | 730 | 640 | | | | 10.3 | 12.4 | |
| | $Grt_{25-27}^{m}$ | | $Pl_{21}$ | *Prg-Hbl* | | | 710 | 645 | | | | 8.2 |
| V-10-1 | $Grt_{27}^{c}$ | $Omp_{29}^{c}$ | | | 750 | 660 | | | 14.0 | | | |
| | $Grt_{24}^{imd}$ | $Di_{19}^{m}$ | | | 715 | 635 | | | 12.0 | | | |
| | $Grt_{24}^{m}$ | $Di_{13}^{m}$ | $Pl_{18}^{s}$ | | 715 | 630 | | | 11.0 | 11.8 | 13.6 | |
| | $Grt_{21}^{m'}$ | $Di_{13}^{m}$ | $Pl_{18}^{s}$ | | 640 | 550 | | | 9.9 | 9.4 | 11.2 | |
| | | | $Pl_{19}$ | *Ed-Hbl* | | | 630 | | | | | 6.7 |
| V-7-2 | $Grt_{30}^{hom}$ | $Omp_{22}^{c}$ | | | 840 | 760 | | | 14.4 | 14.4 | 16.5 | |
| | $Grt_{30}^{m}$ | | $Pl_{20}$ | *Prg-Hbl* | | | 710 | 700 | | | | 7.2 |

Note: Geothermometers: (1) (Powell, 1985); (2) (Ai, 1994); (3) (Holland and Blundy, 1994); (4) Lavrent'eva and Perchuk, 1989). Geobarometers: (5) (Holland, 1980); (6) (Perkins and Newton, 1981); (7) (Eckert *et al.*, 1991); (8) (Blundy and Holland, 1990). Temperatures and pressures were determined accurate to ±40–50°C and 1 kbar, respectively. See Table 3 for abbreviation explanations.

relatively low *Prp* content (22%) at an elevated concentration of *Grs* (30%) (Table 3, Fig. 13). The garnets either preserved their original homogeneity during the retrograde stage or were overgrown with outermost retrograde rims with relatively low *Prp* contents (Fig. 13). The *Grs* concentration is also prone to slightly decrease, although these values in the garnet of sample V-3-1 somewhat increase. The garnets of sample V-10-1 have either a simple (c ⟶ m) or a more complicated (c ⟶ i ⟶ m) zoning, which seems to provide evidence of the compositional variations of the garnet during different decompressional stages. The marginal

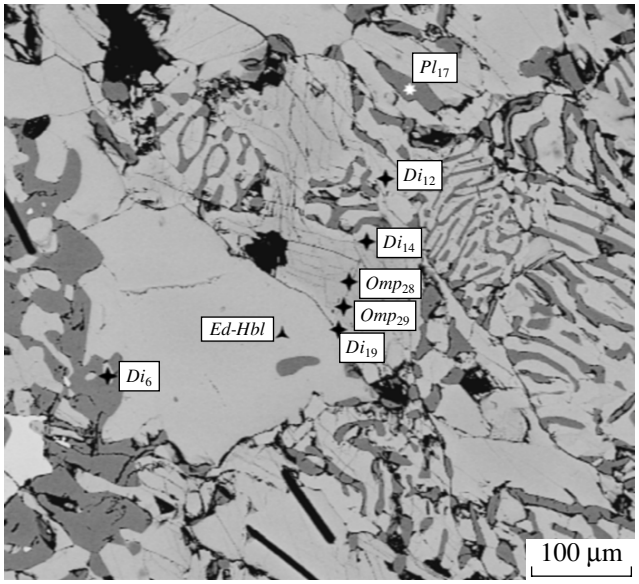


**Fig. 11.** Retrograde zoning in omphacite with the transition to *Cpx–Pl* symplectite. Combinations of decompresional stages I and II. Thin section V-10-1. Back-scattered image.

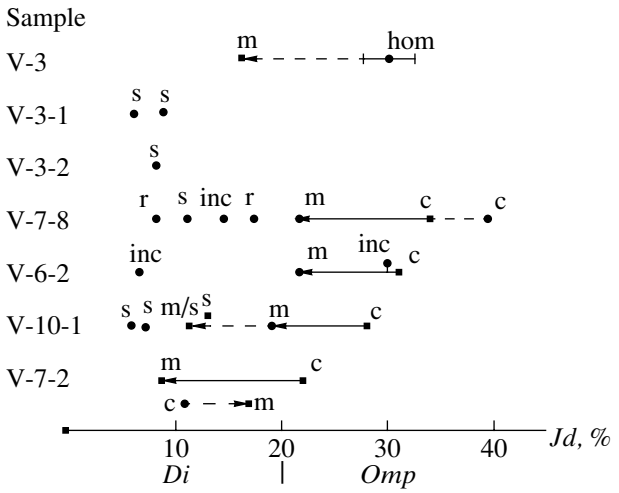


**Fig. 12.** Composition of clinopyroxene of the diopside–jadeite series from the Archean eclogites and symplectitic apoeclogites. The clinopyroxene nomenclature is after (Morimoto, 1988), abbreviations are the same as in Table 3.

zones of crystals with a simple zoning compositionally correspond to the intermediate zones of crystals with a complicate zoning.

Except the relict magmatic bytownite (85% *An* in sample V-3-1, Table 3), plagioclase in the Belomorian eclogites was produced mostly during the retrograde transformations and occurs as interstitial aggregates and in symplectites with *Cpx* or, sometimes, with edenitic amphibole. The plagioclase corresponds to oligoclase (17–23% *An* with a minimum of 14% *An*). However, sample V-3-1 likely contains two populations of andesine: with 47 and 40% *An* (Tables 3, 4). Another plagioclase population (17–25% *An*) occurs in association with *Prg* or *Ed-Hbl* (Table 3, analyses 31, 44, 45). Newly formed plagioclase (20% *An*) was also found in symplectitic aggregates with biotite (Table 3, analyses 45, 46).

The amphibole of these rocks is mostly pargasitic hornblende (or, sometimes, pargasite), edenitic hornblende, and edenite (Fig. 10). Edenite and, more rarely, edenitic hornblende were formed during the decompresional transformations of the eclogites, usually in association with diopside with 6–8% *Jd*. Most of the amphiboles are *Prg-Hbl*, *Prg*, and *Ed-Hbl* of brownish green color, which were formed later, simultaneously with the onset of their crystallization in the *Grt–Cpx* and *Grt* amphibolites. Relatively homogeneous anhedral, subhedral, or euhedral amphibole crystals develop after the *Cpx–Pl* symplectitic groundmass of the rock, preferably at its contacts with *Grt* grains with the gradual replacement of the latter (Fig. 7). The amphibole is zonal (Table 3, analyses 32–33 and 66–67, Fig. 10) with a general compositional trend from *Ed* to *Ed-Hbl* and *Prg-Hbl*.

The *P–T* parameters of the eclogite metamorphism and individual stages of decompression were constrained using the geothermometers and geobarometers of the TPF computer package, developed at the Institute of Experimental Mineralogy, Russian Academy of Sciences, by V.I. Fonarev, A.A. Grafchikov, and A.N. Konilov. In determining the temperatures, we compared the values calculated by different versions of the *Grt–Cpx* thermometer (Powell, 1985; Ai, 1994) (Table 4). The *P–T* diagram for the prograde and retrograde metamorphism of the Archean Belomorian eclogites (Fig. 14) was constructed based on the estimates according to (Powell, 1985), because they seemed to be more realistic, particularly for the late stages of the development of the symplectitic apoeclogites, whose metamorphic parameters seem to be closer to the amphibolite rather than the epidote-amphibolite facies (Table 4: 640°C, after Powell, 1985 and 550°C, after Ai, 1994, respectively), judging from the general analysis of the regional metamorphic evolution (Volodichev, 1990).

The pressure of the *Grt–Cpx* and *Grt–Cpx–Pl–Qtz* assemblages (with *Cpx* containing 9–40% *Jd*) was evaluated by *Jd* compositional isopleths in *Cpx* (Holland, 1980) using temperatures calculated by the *Grt–Cpx* thermometer (Powell, 1985). For the *Pl*- and *Qtz*-bearing assemblages, we compared the data obtained by the isopleth method (Holland, 1980) and by different versions of the *Grt–Cpx–Pl–Qtz* geobarometers (Perkins and Newton, 1981; Eckert *et al.*, 1991). As it turned out, the pressure evaluations according to (Perkins and Newton, 1981) were the most consistent with the values read from the *Jd* isopleths (Holland, 1980), while the data according to (Eckert *et al.*, 1991) were relative overestimates (Table 4). Because of this, in constructing the *P–T* diagram (Fig. 14) for the *Pl*- and *Qtz*-bearing assemblages, we utilized data of the *Grt–Cpx–Pl–*

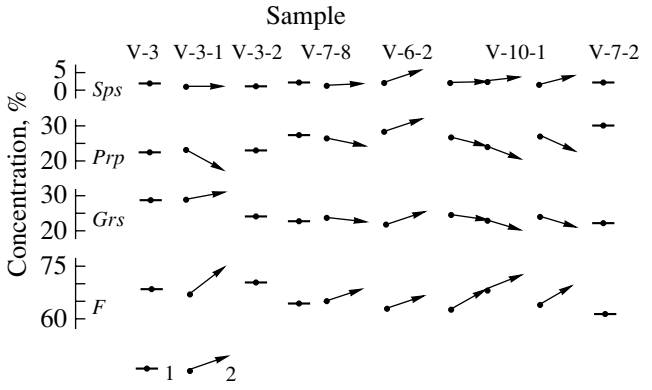


**Fig. 13.** Composition of (1) homogeneous and (2) zonal garnet grains from the Archean eclogites and symplectitic apoeclogites. Vectors 2 determine the compositional variations in garnet grains from their cores to margins, $F$ = Fe/(Fe + Mg) × 100.

*Qtz* geobarometer (Perkins and Newton, 1981) with regard for the temperatures evaluated by the *Grt–Cpx* geothermometer (Powell, 1985).

The *P–T* parameters of metamorphism of the amphibole-bearing assemblages were quantified by the *Hbl–Pl*–quartz geothermometer (Holland and Blundy, 1994). When there was no doubt in the equilibrium relations between the amphibole and garnet, the temperatures were determined by the *Grt–Hbl* thermometer (Lavrent'eva and Perchuk, 1989). For the same amphibole grains, the temperature values determined by these thermometers differ (Table 4), so that the *P–T* diagram (Fig. 14) shows the data obtained with both geothermometers (the dashed lines mark the temperature intervals). The *Grt–Hbl–Pl–Qtz* geobarometer (Kohn and Spear, 1990) commonly used to evaluate pressures at such complexes (Korikovsky and Hovorka, 2001; and others) is inapplicable to our rocks because the amphibole contains >0.6 f.u. of Na, so that we determined pressures for *Ed-Hbl* and *Prg-Hbl* by the *Hbl* geobarometer (Blundy and Holland, 1990).

The data thus obtained (Table 4, Fig. 14) are mostly well consistent, except only for one value: an obvious temperature overestimate of 850°C at $P$ = 11.4 kbar for sample V-3-1, for the assemblage of $Grt^{23} - Di_9 - Pl_{47}$.

The eclogites proper are bimineralic $Grt^{27-28}_{22-25}$ or $Grt^{21-22}_{28-30}$ (sample V-3) and $Omp_{28-40}$ rocks. The variations in the chemistry of minerals and, correspondingly, the *P–T* parameters of their crystallization (Table 4) seem to have been controlled by different stages of the prograde eclogitization process, which evolved from $T$ = 740°C at $P$ = 14.2 kbar (sample V-3) to $T$ = 865°C at $P$ = 17.5 kbar (sample V-7-8) (Fig. 14, Table 4). The mineral assemblages of the eclogites became unstable, and the rocks were affected by extensive decompressional transformations. The process was continuous and can be subdivided into stages according to the discrete groups of decreasing *Jd* contents in the clinopyroxene. There were four stages of eclogite transformations with the development of symplectitic apoeclogites (I–III) and garnet–clinopyroxene amphibolites (IV). Stages I, II, and IV are pronounced most clearly, with the boundary between stages II and III determined provisionally.

Stage I was characterized by "slow" decompression with a gradual decrease in the *Jd* content to $Omp_{21}$ (or even to $Di_{19}$ and $Di_{16}$ in some samples) in the margins of clinopyroxene crystals. The compensation product of this change (plagioclase in the form of chains of small grains in the interstices of clinopyroxene grains, Fig. 8) was produced under similar conditions. The mineral assemblage of stage I is $Grt^{24-30}_{21-23}$–($Omp_{22}$–$Di_{19}$)–$Pl_{17-18}$. The process occurred as the pressure decreased from 14.4 to 12.0 kbar at $T$ = 715–780°C (Fig. 14, Table 4).

The kinetics of stage II of the decompression process seems to have been "fast". The omphacite decomposed into $Di_{9-13}$ and $Pl_{17-22}$, up to $Pl_{47}$, with the development of symplectites of the dactylitic or lamellar types (Joanny *et al.*, 1991; Fig. 9) at $P$ = 12–11 kbar and $T$ = 715–765 (855?)°C. The mineral assemblage of this stage was $Grt^{23-24}_{23-24(29)}$–$Di_{9-13}$–$Pl_{17-22(47)}$.

Stage III was marked by transformations of the symplectites, with the broadening of the lamellae and transitions to the globular type, although thin lamellae with such *Cpx–Pl* relations still occur in some samples. Plagioclase in sample V-10-1 occurs in aggregates not only with $Di_7$ but also with edenite. Late during this stage, other amphiboles started to crystallize: these were Fe-rich pargasite and Fe-rich pargasitic or edenitic hornblende in association with garnet and clinopyroxene. This process marked the eclogite–amphibolite transition. The mineral assemblages of stage III are $Grt^{18-25}_{21-24(29)}$–$Di_{5-8}$–$Pl_{19-24(40)}$ ± *Am*, *Bt*. The metamorphic conditions corresponded to $P$ = 10.3–8.5 kbar at $T$ = 710–730°C.

Stage IV was responsible mostly for the formation of garnet–clinopyroxene and garnet amphibolites with the assemblages $Grt^{17-21}_{28-23}$–*Hbl*–$Pl_{19-25} \pm Di_{<5}$. Amphibole became the main rock-forming mineral, and the clinopyroxene and plagioclase still retain traces of a modified symplectitic structure of the globular type. The metamorphic conditions were $P$ = 8.2–6.5 kbar, $T$ = 630–715°C (Table 4). This stage was marked by intense deformations with the origin of narrow isoclinal folds in the banded eclogite-like rocks and garnet amphibolites.

The slope of the *P–T* decompression trajectory is relatively steep, with a low temperature gradient at a significant pressure decrease (Fig. 14).

## DISCUSSION

The eclogite relics found near the village of Gridino occur in an association of rocks of different composition and genetic nature, which were produced at different depths, i.e., are components of an allochthonous mixture, most probably, in a tectonic melange zone. Later extension and decompression impregnated this zone by granitic material of tonalite–plagiogranite composition (judging from enderbite relics) at granulite-facies depths. This process gave rise to a complicated polygenetic chaotic rock complex, whose morphology and composition are most close to migmatites of the agmatite type.

The protolith of the eclogites consisted of mafic and ultramafic rocks, whose petrochemistry was comparable with that of analogous rocks of the ophiolite-like complex in the central Belomorian Mafic Zone of the BMB (Slabunov and Stepanov, 1998; Bibikova *et al.*, 1999). Petrologically interesting rocks are the anchimonomineralic zoisite varieties, which seem to have developed, along with eclogites, after anorthosites under eclogite-facies conditions.

The chemistry of minerals and *P–T* parameters of the Archean crustal eclogites in the BMB correspond to the eclogite metamorphic facies (Miyashiro, 1973; Dobretsov *et al.*, 1989; Closs, 1993; and others) of relatively insignificant depth. These *P–T* parameters of prograde eclogite metamorphism allow both the rare preservation of the pre-eclogite plagioclase (sample V-3-1) and the possible occurrence of plagioclase in association with *Grt*, *Cpx* ± *Am* (given some uncertainties in the petrographic relations between *Cpx* and *Pl* in sample V-7-2) during the relatively low-temperature stage. However, the bulk of plagioclase contained in the BMB eclogites still seems to have been produced by decompression processes. The mineral assemblages of stage I of decompression have metamorphic parameters analogous to the plagioclase-eclogite subfacies of the eclogite facies, which was distinguished by Korikovsky (2002) for temperatures of 400–700°C. The *P–T* parameters of stages II and III corresponded to the high-pressure granulite facies: mafic garnet granulites (Cloos, 1993). These parameters of stage IV corresponded to the HP amphibolite–granulite facies (Fig. 14).

The eclogites have variable compositions of their minerals and metamorphic *P–T* conditions, perhaps, because they were formed at different depths. Considered collectively, these rocks define a prograde evolutionary trend with the *P–T* conditions varying within the ranges of $P$ = 14.0–17.5 kbar and $T$ = 740–865°C (which corresponded to the geotherms 12–13°C/km). These geotherms coincide with the trend of the moderate Archean geothermal gradient (Martin, 1986), whose realism is, thus, confirmed for the evolution of the processes that produced the Archean crust. This fact predetermines the possibility of subduction processes during this period for a "warm" plate (Peacock, 1993) (Fig. 14).

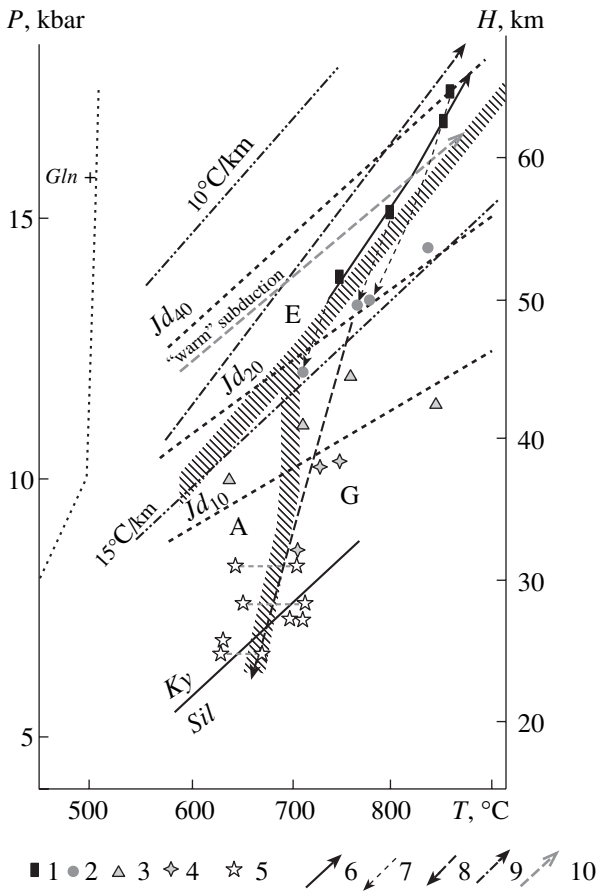


**Fig. 14.** *P–T* parameters of the prograde and retrograde metamorphism of Archean eclogites in the BMB.

(1–5) *P–T* parameters of (1) eclogites; (2) symplectitic apoeclogites I; (3) symplectitic apoeclogites II; (4) symplectitic apoeclogites III (I–III—decompressional stages); (5) garnet–clinopyroxene amphibolites of decompressional stage IV; (6) prograde metamorphic *P–T* path of the eclogites; (7) retrograde *P–T* metamorphic trajectory for stage-I "slow" decompression (for individual samples); (8) generalized retrograde *P–T* trajectory for the eclogites during stages I–IV; (9) Archean moderate geothermal gradient (Martin, 1986); (10) "warm" subduction geotherm (Peacock, 1993). The compositional isopleths of *Jd* in *Cpx* are given after (Holland, 1998), the *Ky–Sil* line is after (Holland and Powell, 1990), the *Gln* stability field is after (Maresh, 1977); the boundaries of the (E) eclogite, (G) granulite, and (A) amphibolite facies are after (Cloos, 1993).

Another distinctive feature of the Archean granulites that makes them similar to Phanerozoic granulites is the multistage retrograde decompressional transformations of the eclogites in the regime of subisothermal decompression. In the continuous (prograde and retrograde) clockwise *P–T* trajectory, which was controlled by changes in the geodynamic environments of subsidence and exhumation, the decompressional stage corresponded to the gradual exhumation of the eclogites. The *P–T* conditions of the retrograde decompressional transformations of the BMB eclogites are quite similar to those of Phanerozoic eclogites in the Scandinavian

Caledonides (Seve Nappe Complex) and these rocks in the French Massif Central (Mercier *et al.*, 1991).

A problem of principal importance discussed in this paper is the Archean age of the eclogites. The geological and geochronological evidence presented above seems to be sufficient to confirm an Archean age of the rocks.

It is also pertinent to mention that the possibility that these eclogites were produced by the overprinted Early Proterozoic HP metamorphism (at ~2.45 Ga) (see above) can be disregarded, because the rocks of the early Proterozoic lherzolite–gabbronorite complex to which eclogite metamorphism was related cut across the eclogites that had already been retrogressed to garnet–clinopyroxene amphibolites with relict symplectitic textures. At the same time, the process of Early Proterozoic eclogitization generally did not attain the *P–T* conditions of the Archean eclogites even during the metamorphic culmination. This fully pertains to the sampling sites of the Archean eclogites (sample V-6-2 from Izbnaya Luda Island, sample V-7-8 from Second Kokkov Island, and sample V-10-1 from Vorotnaya Luda Island), where crosscutting gabbronorite dikes show very insignificant traces of eclogitization, which manifests itself only as locally occurring kelyphitic and coronitic *Grt–Cpx* reaction rims.

Thus, the BMB eclogites from the vicinity of the village of Gridino are likely the world's first confirmed find of Late Archean crustal eclogites. This implies that a thick (~60–65 km, Fig. 14) crust should have existed in the Archean to make it possible the occurrence of convergent plate-tectonic processes of subduction and collision. As follows from the *P–T* parameters of the eclogite metamorphism, the former process occurred at a "warm" plate. It is still unclear as to what was the geodynamic environment in which the Gridino Archean eclogites were produced and whether their genesis was related to one of these processes or they are exhumed lower crustal fragments. These issues will, hopefully, be clarified by further detailed geological–petrological and geochronological research.

## PRINCIPAL CONCLUSIONS

(1) The eclogites and the products of their decompressional retrogression (symplectitic apoeclogites or eclogite-like rocks) were found and examined in Belomorian Mobile Belt of the Baltic Shield near the village of Gridino. These rocks were dated on zircon at 2720 ± 8 Ma and, thus, are the world's first confirmed find of Late Archean crustal eclogites.

(2) The eclogite-bearing Archean complex consists of extensively migmatized rocks of a tectonic melange zone. The granitoid constituent of the migmatites has a tonalite–plagiogranite composition and was produced, judging from enderbite relics, under granulite-facies conditions, at multistage overprinted deformations and metamorphism, which transformed these rocks into gneisses. The eclogites are components of an allochthonous mixture of paleosome fragments, which compose an association of strongly disintegrated and displaced fragments of rocks having different compositions and genetic nature and produced at different depths. This suggests that the granitoid material was emplaced (migmatization) into a preexisting zone of tectonic melange.

(3) The protolith of the eclogites consisted of mafic and more rare ultramafic (pyroxenites) rocks, whose petrochemical characteristics are comparable with those of the ophiolite-like mafic complex in the Central Belomorian Mafic Zone.

(4) The Archean eclogites were produced at $P = 14.0$–$17.5$ kbar and $T = 740$–$865$°C at depths of 60–65 km, which allow the occurrence of "warm" subduction.

(5) The eclogites occur as relics among symplectitic apoeclogites (eclogite-like rocks) and garnet–clinopyroxene amphibolites, which replaced the eclogites during retrograde decompression. The evolutionary trajectory of the multistage subisothermal decompression spans ranges of 13.0–14.0 to 6.5 kbar and $T = 770$–$650$°C during the exhumation of the eclogites.

## ACKNOWLEDGMENTS

The authors thank Prof. L.L. Perchuk and O.V. Parfenova (Moscow State University) for the possibility of analyzing minerals on a microprobe. M. Whitehouse (Sweden) is thanked for assistance in geochronological dating on a NORDSIM ion microprobe. We appreciate consultations with V.S. Stepanov (Institute of Geology, Karelian Research Center, Russian Academy of Sciences) and thank him for the factual materials provided for this research. Corresponding member of the Russian Academy of Sciences S.P. Korikovsky (Institute of the Geology of Ore Deposits, Petrography, Mineralogy, and Geochemistry, Russian Academy of Sciences) is thanked for valuable comments and constructive criticism during the preparation of the manuscript. This study was supported by the Russian Foundation for Basic Research (project nos. 00-05-64295, 03-05-64010, and 03-05-65051).

## REFERENCES

1. Y. A. Ai, "A revision of the Garnet-Clinopyroxene $Fe^{2+}$–Mg Exchange Geothermometer," Contrib. Mineral. Petrol. **115** (4), 467–473 (1994).
2. A. R. Alderman, "Eclogites from the Vicinity of Glenelg, Jnverness-Shire," Q. J. Geol. Soc. London **92**, 488–533 (1936).
3. A. J. Baer, "Speculations on the Evolution of the Lithosphere," Precambrian Res. **5** (3), 249–260 (1977).
4. E. V. Bibikova, *Uranium–Lead Geochronology for Early Evolution Stages of Ancient Shields* (Nauka, Moscow, 1989) [in Russian].
5. E. V. Bibikova, A. I. Slabunov, S. V. Bogdanova, *et al.*, "Early Magmatism of the Belomorian Mobile Belt,

Baltic Shield: Lateral Zoning and Isotopic Age," Petrologiya **7** (2), 115–140 (1999) [Petrology **7** (2), 123–146 (1999)].

6. J. D. Blundy and T. J. B. Holland, "Calcic Amphibole Equilibria and a New Amphibole–Plagioclase Geothermometer," Contrib. Mineral. Petrol. **104** (2), 208–224 (1990).
7. R. G. Cawthorn and K. D. Collerson, "The Recalculation of Pyroxene End-Member Parameters and the Estimation of Ferrous and Ferric Iron Content from Electron Microprobe Analyses," Am. Mineral. **59** (11–12), 1203–1208 (1974).
8. J. M. Cebria, "PX: A Program for Pyroxene Classification and Calculation of End-Members," Am. Mineral. **75**, 1426–1427 (1990).
9. M. Cloos, "Lithospheric Buoyancy and Collisional Orogenesis: Subduction of Oceanic Plateaus, Continental Margins, Island Areas, Spreading Ridges, and Seamounts," Geol. Soc. Am. Bull. **105** (6), 715–737 (1993).
10. N. L. Dobretsov, N. V. Sobolev, and V. S. Shatskii, *Eclogites and Glaucophane Schists in Folded Belts* (Nauka, Novosibirsk, 1989) [in Russian].
11. J. O. Eckert, Jr., R. C. Newton, and O. J. Kleppa, "The ΔH of Reaction and Recalibration of Garnet–Pyroxene–Plagioclase–Quartz Geobarometers in the CMAS System by Solution Calorimetry," Am. Mineral. **76** (1/2), 148–160 (1991).
12. G. Godard, "Eclogites and Their Geodynamic Interpretation: A History," J. Geodynam., No. 32, 165–203 (2001).
13. D. H. Green, "Genesis of Archean Peridotitic Magmas and Constraints on Archean Geothermal Gradients and Tectonics," Geology **3**, 15–18 (1975).
14. T. J. B. Holland, "The Reaction Albite = Jadeite + Quartz Determined Experimentally in the Range 600–1200 Grad. C," Am. Mineral. **65**, 129–134 (1980).
15. T. J. B. Holland and J. D. Blundy, "Non-Ideal Interactions in Calcic Amphiboles and Their Bearing on Amphibole–Plagioclase Thermometry," Contrib. Mineral. Petrol. **116**, 433–447 (1994).
16. T. J. B. Holland and R. Powell, "An Enlarged and Updated Internally Consistent Thermodynamic Dataset with Uncertainties and Corrections: The System $K_2O$–$Na_2O$–CaO–MgO–MnO–FeO–$Fe_2O_3$–$Al_2O_3$–$TiO_2$–$SiO_2$–C–$H_2$–$O_2$," J. Metamorphic Geol. **8**, 89–124 (1990).
17. V. Joanny, H. van Roermund, and J. M. Lardeaux, "The Clinopyroxene/Plagioclase Symplectite in Retrograde Eclogites: A Potential Geothermobarometer," Geol. Rundsch. **80** (2), 303–320 (1991).
18. M. Y. Kohn and F. S. Spear, "Two New Geobarometers for Garnet Amphibolites, with Applications to Southeastern Vermont," Am. Mineral. **75** (1/2), 89–96 (1990).
19. S. P. Korikovsky and D. Hovorka, "Two Types of Garnet–Clinopyroxene–Plagioclase Metabasites in the Mala Fatra Mountains Crystalline Complex, Western Carpathians: Metamorphic Evolution, *P–T* Conditions, Symplectitic and Kelyphitic Textures," Petrologiya **9** (2), 140–166 (2001) [Petrology **9** (2), 119–141 (2001)].
20. S. P. Korikovsky, "Facies of Deep Crustal Eclogites," in *Proceedings of All-Russian Scientific Conference "Geology and Geochemistry at the Turn of the 20th and 21th Centuries"* (Moscow, 2002), Vol. 2, pp. 108–110 [in Russian].
21. S. P. Korikovsky, V. Mircovski, and G. S. Zakariadze, "Metamorphic Evolution and the Composition of the Protolith of Plagioclase-Bearing Eclogite–Amphibolites of the Buchim Block of the Serbo-Macedonian Massif, Macedonia," Petrologiya **5** (6), 596–613 (1997) [Petrology **5** (6), 534–549 (1997)].
22. T. E. Krogh, "A Low-Contamination Method for Hydrothermal Decomposition of Zircon and Extraction of U and Pb for Isotopic Age Determinations," Geochim. Cosmochim. Acta **37**, 485–494 (1973).
23. I. V. Lavrent'eva and L. L. Perchuk, "An Experimental Study of the Amphibole–Garnet Equilibrium: Calcium-Free System," Dokl. Akad. Nauk SSSR **306** (1), 173–175 (1989).
24. B. E. Leak, "Nomenclature of Amphiboles," Am. Mineral. **63** (11–12), 1023–1053 (1978).
25. S. B. Lobach-Zhuchenko, N. A. Arestova, V. P. Chekulaev, *et al.*, "Geochemistry and Petrology of 2.40–2.45 Ga Magmatic Rocks in the North-Western Belomorian Belt, Fennoscandian Shield, Russia," Precambrian Res. **92**, 223–250 (1998).
26. K. B. Ludwig, "ISOPLOT Program," USA Geol. Surv. Open-File Rep., No. 91 (1991).
27. W. V. Maresh, "Experimental Studies on Glaucophane: An Analysis of Present Knowledge," Tectonophysics **43**, 109–125 (1977).
28. H. Martin, "Effect of Steeper Archean Geothermal Gradient on Geochemistry of Subduction-Zone Magmas," Geology **14**, 753–756 (1986).
29. M. Masamichi and T. Hi, "Prediction of Crystal Structures of Minerals under Extremal Conditions by Methods of Energy Minimization," J. Mineral. Soc. Jpn. **16**, 217–221 (1983).
30. A. Mattana and A. D. Edgar, "The Significance of Amphibole Compositions in the Genesis of Eclogites," Lithos **3**, 37–49 (1969).
31. L. Mercier, H. van Roermund, and J. M. Lardeaux, "Comparison of *P–T–t* Paths in Allochthonous High Pressure Metamorphic Terrains from the Scandinavian Caledonides and the French Central Massif: Contrasted Thermal Structures during Uplift," Geol. Rundschau **80** (2), 333–348 (1991).
32. A. Miyashiro, *Metamorphism and Metamorphic Belts* (Wiley, New York, 1973).
33. N. Morimoto, "Nomenclature of Pyroxene," Mineral. Mag. **52** (4), 535–550 (1988).
34. S. M. Peacock, "The Importance of Blueschist–Eclogite Dehydration Reactions in Subducting Oceanic Crust," Geol. Soc. Am. Bull. **105** (5), 684–694 (1993).
35. J. A. Percival, "Archean High-Grade Metamorphism," in *Archean Crustal Evolution: Development in Precambrian Geology* (Elsevier, New York, 1994), pp. 357–410.
36. D. Perkins III and R. C. Newton, "Charnockite Geobarometers Based on Coexisting Garnet–Pyroxene–Plagioclase–Quartz," Nature **292** (9), 144–146 (1981).
37. R. Powell, "Regression Diagnostics and Robust Regression in Geothermometer/Geobarometer Calibration: The Garnet–Clinopyroxene Geothermometer Revised," J. Metamorp. Geol. **3** (3), 231–243 (1985).

38. M. Sanborn-Barrie, S. D. Carr, and R. Theriault, "Geochronological Constraints on Metamorphism, Magmatism, and Exhumation of Deep Crustal Rocks of the Kramanituar Complex, with Implications for the Paleoproterozoic Evolution of the Archean Western Churchill Province, Canada," Contrib. Mineral. Petrol. **141**, 592–612 (2001).
39. A. I. Slabunov and V. S. Stepanov, "Late Archean Ophiolites of the Belomorian Mobile Belt, Fennoscandian/Baltic Shield: Why not?" in *Abstracts of Papers of International Ophiolite Symposium and Field Excursion "Generation and Emplacement of Ophiolites through Time," August 10–15, 1998, Oulu, Finland* (Geol. Surv. Finland, 1998), Spec. Pap. 26, p. 56.
40. A. I. Slabunov, A. N. Larionov, E. V. Bibikova, *et al.*, "The Geology and Geochronology of the Shobozero Massif, the Lherzolite–Gabbro–Norite Complex of the Belomorian Mobile Belt," in *The Geology and Minerals of Karelia* (Petrozavodsk, 2001), No. 3, pp. 3–14 [in Russian].
41. J. S. Stacey and J. D. Kramers, "Approximation of Terrestrial Lead Isotope Evolution by a Two-Stage Model," Earth Planet. Sci. Lett. **26**, 207–221 (1975).
42. V. S. Stepanov, "Magmatites at Gridino Valley: Chemical and Mineralogical Compositions, Formation Sequence, and Some Evolutionary Features," in *The Precambrian in Northern Karelia* (Karel. Fil. Akad. Nauk SSSR, Petrozavodsk, 1990), pp. 78–101 [in Russian].
43. C. D. Storey, T. S. Brewer, and R. R. Parrish, "Grenvillian Age Decompression of Eclogites in the Glenelg–Attadale Inlier, NW Scotland," Geophys. Res. Abstracts **5**, 06080 (2003).
44. S. S. Sun, "Chemical Composition and Origin of the Earth's Primitive Mantle," Geochim. Cosmochim. Acta **46**, 179–192 (1982).
45. O. I. Volodichev, "Metamorphic Evolution of the Polycyclic Belomorian Complex," in *Recurrence and Direction of Regional Metamorphism* (Nauka, Leningrad, 1977), pp. 57–79 [in Russian].
46. O. I. Volodichev, "Geological and Petrological Traces of the Subduction Stage of the Belomorian Collision Structure in the Late Archean," in *Proceedings of International Conference "Belomorian Mobile Belt"* (Petrozavodsk, 1997), pp. 23–24 [in Russian].
47. O. I. Volodichev, *Belomorian Complexes of Karelia* (Nauka, Leningrad, 1990) [in Russian].
48. M. Whitehouse, S. Claesson, T. Sunde, and J. Vestin, "Ion Microprobe U–Pb Zircon Geochronology and Correlation of Archean Gneisses from the Lewisian Complex of Gruinard Bay, Northwestern Scotland," Geochim. Cosmochim. Acta **61**, 4429–4438 (1997).
49. M. Wiedenbeck, F. Corfu, W. L. Griffin, *et al.*, "Three Natural Zircon Standards for U–Th–Pb, Lu–Hf, Trace Element, and REE Analysis," Geostand. Newsl. **19**, 1–23 (1995).